

The copyright of this thesis vests in the author. No quotation from it or information derived from it is to be published without full acknowledgement of the source. The thesis is to be used for private study or non-commercial research purposes only.

Published by the University of Cape Town (UCT) in terms of the non-exclusive license granted to UCT by the author.

OPERATION OF INDUCTION MACHINES IN THE PRESENCE OF UNBALANCED SUPPLIES



BY

Marubini J. Manyage

Department of Electrical Engineering
University of Cape Town

FOR

Professor Pragasen Pillay

Machines and Drives Professor
Department of Electrical Engineering
University of Cape Town

Thesis prepared in fulfillment of the requirements for Masters of Science degree
in Electrical Engineering at the University of Cape Town.

December 2001

DECLARATION

I, Marubini J. Manyage, submit this thesis in fulfillment of the requirements for Masters of Science degree in Electrical Engineering at the University of Cape Town. I claim that this is my work and has not been submitted in any other University. All the work from other sources are referenced accordingly.

Signature:...

Signed by candidate

Date:.....

Marubini J. Manyage

ACKNOWLEDGEMENTS

The Author wishes to thank God and the following people for their assistance received during the course of this project.

- Professor Pragasen Pillay, for his supervision, guidance and positive suggestions throughout the project.
- Professor S. G. McLaren, for sharing his expertise and constructive criticism towards the project.
- UCT Machines Group: S. Khumalo, A. Khan, H. Douglas, T. Mthombeni, D Johnson and C. Wozniak, for the technical support.
- My family, for their unconditional love and moral support.
- My friends: Julia, Mphedziseni, Mashudu, Bishop, Rofhiwa, Ashley, Jane, Nkhumeleni, Ntsandeni and Xolani, for their encouragement throughout the project.
- H. Mostert, for his assistance received near the end of this project.
- ESKOM, for their financial support.

TERMS OF REFERENCE

This project was proposed by Prof. Pragasen Pillay, Electrical Machines and Drives professor at the University of Cape Town, on 03 January 2001. The purpose of the project was to determine and to restore the life of three-phase induction motor when supplied with a combination of overvoltage or undervoltage with unbalanced voltages. Professor Pillay specific instructions were:

1. To do a literature survey on the effects of voltage unbalance, thermal models, motor derating and motor life.
2. To study and compare the available definitions of voltage unbalance.
3. To develop electrical and thermal models based on motor testing.
4. To predict motor life when the motor is operating with a combination of over or undervoltages with unbalanced voltages.
5. To develop a new derating curve which includes a combination of over and undervoltages with unbalanced voltages, in order to restore motor life.

SYNOPSIS

Three-phase induction machines are widely used in South Africa for industrial, commercial and residential applications because of their simple construction and low maintenance. The manufacturers design these motors to provide their nameplate ratings when supplied with balanced sinusoidal voltages. However, the power system experiences unbalanced voltages, overvoltages, undervoltages, etc, which are seen at the motor terminals.

The South African Electricity Supply Utility (Eskom) supplies the commercial and industrial systems with a line voltage range of $400V \pm 10\%$. An Induction motor rated at 380V or 400V will therefore experience overvoltages or undervoltages depending on the location of the motor from the supply.

Besides overvoltages and undervoltages, unbalanced voltages exist on the power system. The tolerable level of voltage unbalance on the South African three-phase networks is 2%, and may be up to 3% in the rural areas. In practice, induction motors experience a combination of overvoltages or undervoltages with unbalanced voltages. This affects motor life.

NEMA has done research on induction motors operating under unbalanced voltages. They defined voltage unbalance and produced a derating curve, assuming the average voltage applied to the motor is equal to the rated voltage. The IEC has another definition of voltage unbalance based on the positive and negative sequence voltages. The IEC definition is referred to as the true definition. Two formulas that approximate the true definition also exist. An analysis was done in order to understand the implications of using these

definitions of voltage unbalance in the South African power system. It was found that the NEMA definition and the true definition do not differ significantly below a 5% unbalance.

In order to estimate motor life when a motor is supplied with unbalanced voltages, in combination with over or undervoltages, electrical and thermal models were developed to predict the temperature. The electrical model was based on the positive and negative sequence equivalent circuits. The thermal model used, separated stator and rotor thermal circuits. The thermal parameters were obtained from simple tests rather than from motor design data. The predicted temperature values agree closely to the measured values.

The interaction between the electrical model, thermal model and the thermal ageing equation were used to estimate motor life when the motor is supplied with unbalanced voltages, in combination with over or undervoltages. Motor life is reduced when the operating temperature exceeds the rated. In order to restore motor life, new derating curves were developed since the NEMA derating curve is limited to rated average voltage. Motor life can be restored by applying the new derating curves developed here.

TABLE OF CONTENTS

SECTION	PAGE
Acknowledgements	i
Terms of reference	ii
Synopsis.....	iii
List of figures	viii
List of tables	x
Nomenclature	xi
Chapter 1: INTRODUCTION	1
1.1 Overview.....	1
1.2 Research Background.....	1
1.3 Literature Survey on the effects of voltage unbalance on Induction Machines	3
1.3.1 Symmetrical Components.....	3
1.3.2 Effects of Voltage Unbalance on the Induction Machine.....	5
1.4 Literature Survey on Motor Life.....	8
1.5 Literature Survey on Thermal Models.....	9
1.6 Literature Survey on Relevant Papers	10
1.7 Literature Survey on Motor Derating.....	12
1.8 Summary and Discussion of the Project	13
1.9 Contribution of this Thesis	13

TABLE OF CONTENTS

SECTION	PAGE
Chapter 2: DEFINITION OF VOLTAGE UNBALANCE	15
2.1 Introduction	15
2.2 Definitions of Voltage Unbalance	15
2.2.1 NEMA Definition.....	15
2.2.2 IEEE Definition.....	16
2.2.3 IEC Definition.....	16
2.2.4 Approximation Formula.....	17
2.3 Analysis of the Definitions of Voltage Unbalance.....	17
2.4 Comparison of NEMA Definition and True definition of Voltage Unbalance.....	23
2.5 Conclusions	25
Chapter 3: ELECTRICAL AND THERMAL MODELS	26
3.1 Introduction	26
3.2 Electrical model of an induction machine	27
3.2.1 Positive and Negative Sequence Equivalent Circuits.....	27
3.2.2 Equivalent Circuit Parameter Determination	28
3.2.3 Motor Performance Characteristics.....	29
3.3 Thermal model of an induction machine	32
3.3.1 Thermal Model Circuits	33
3.3.2 Thermal model circuit analysis.....	34
3.3.3 Thermal Model Circuit Parameter Determination	36
3.3.4 Thermal Model Performance Test.....	41
3.4 Conclusions	47

TABLE OF CONTENTS

SECTION	PAGE
Chapter 4: MOTOR LIFE ESTIMATION AND DERATING	48
4.1 Introduction	48
4.2 Insulation Classes	49
4.3 Thermal Ageing Model	49
4.4 Motor Lifetime Estimation	50
4.4.1 Motor Lifetime Estimation at Rated Condition	50
4.4.2 Motor Lifetime Estimation under Unbalance Supplies.....	52
4.5 Scenarios on Motor Lifetime Estimation	57
4.6 Development of New Derating Curves	62
4.7 Conclusions	64
Chapter 5: CONCLUSIONS AND RECOMMENDATIONS	66
REFERENCE	70
APPENDIX A: EXPERIMENTAL SETUP	75
APPENDIX B: ELECTRICAL MODEL CIRCUIT PARAMETERS	76
APPENDIX C: THERMAL MODEL CIRCUIT PARAMETERS	77
BIOGRAPHY	78

LIST OF FIGURES

Figure 1.1	Positive sequence equivalent circuit	4
Figure 1.2	Negative sequence equivalent circuit	5
Figure 1.3	NEMA derating curve	12
Figure 2.1	Relationship of the definitions of voltage unbalance	20
Figure 2.2	Relationship of the definitions of voltage unbalance with angle variation	22
Figure 2.3	Relationship between the NEMA and the true definitions of voltage unbalance	23
Figure 3.1	Electrical and thermal models flow-chart	26
Figure 3.2	Positive sequence equivalent circuit	27
Figure 3.3	Negative sequence equivalent circuit	28
Figure 3.4	Core loss at rated, 10% overvoltage and undervoltage with unbalanced voltages	30
Figure 3.5	Core loss from 90% -110% average voltages with unbalanced voltages	30
Figure 3.6	Stator thermal model circuit	33
Figure 3.7	Rotor thermal model circuit	34
Figure 3.8	Thermal conductance circuit	38
Figure 3.9	Thermal capacitance circuit	40
Figure 3.10	Thermal model test results under variable loads	43
Figure 3.11	Supply voltage variation with time	46
Figure 3.12	Thermal model test results under supply voltage variation	46
Figure 4.1	Motor life prediction flow-chart	50
Figure 4.2	Balanced voltage waveforms	51
Figure 4.3	5% unbalanced voltage waveforms	53
Figure 4.4	10% overvoltage with 5% unbalanced voltage waveforms	53
Figure 4.5	10% undervoltage with 5% unbalanced voltage waveforms	53
Figure 4.6	Motor winding temperature curves	54
Figure 4.7	Motor winding temperature rise and loss of life curves	55

Figure 4.8 Motor winding temperature change with time.....58
Figure 4.9 Motor winding temperature change within 24 hours.....61
Figure 4.10 Motor derating flow-chart62
Figure 4.11 New derating curves63

APPENDIX

Figure A: Induction motor coupled to a dc generator75
Figure C: Stator thermal model circuit.....77

University of Cape Town

LIST OF TABLES

Table 2.1	Range of voltage unbalance.....	21
Table 3.1	Electrical/Thermal analogies	34
Table 3.2	Thermal model test results under balanced voltages	42
Table 3.3	Thermal model test results under unbalanced voltages	44
Table 3.4	Thermal model test results under over and undervoltages.....	44
Table 4.1	Insulation class ratings.....	49
Table 4.2	Motor winding temperature rise and loss of life.....	56
Table 4.3	Motor voltage and temperature variation with time.....	57
Table 4.4	Deterioration rate and loss of life.....	60

APPENDIX

Table B-1:	No-load and locked rotor tests.....	76
Table B-2:	Positive and negative sequence equivalent circuit parameters	76

NOMENCLATURE

DC = Direct current

IEC = International Electrotechnical Commission

IEEE = Institute of Electrical and Electronics Engineers

NEMA = National Electrical Manufacturers Association

RMS = Root mean square

University of Cape Town

Chapter 1

1. INTRODUCTION

1.1 OVERVIEW

Chapter 1 addresses the objectives of this project. This research is based on the literature survey done on the effects of voltage unbalance on induction machines and motor life reduction. Thermal models and motor derating are also reviewed. Motor life estimation and restoration in the presence of overvoltages and undervoltages with a combination of unbalance voltages are areas that need to be examined, and is therefore the focus of this research.

1.2 RESEARCH BACKGROUND

Three-phase induction motors perform best when supplied by balanced sinusoidal waveforms of the rated value. In practice, the ideal supply conditions are not that easy to achieve. The power system experiences voltage unbalance, overvoltages, undervoltages, voltage dips, harmonics, etc. These distortions in the power system quality can reduce the efficiency and the life span of the motor.

Most of the three-phase induction motors available in South African industries are designed to operate from 380V supplies. The Electricity Supply Utility (Eskom) supplies the commercial and industrial systems with a line voltage range of $400V \pm 10\%$. One of the reasons for this higher voltage is to allow for the cable voltage drop so that the proper voltage at the terminals of the motors can be obtained. This is not always achieved in practice, with the line voltages at the motor terminals being much higher or lower than the rated 380V, depending on the location of the motor and the length of the feeder used.

Voltage unbalance is another problem that has existed on the power system for years and continues to exist today. Voltage unbalance is described as an inequality in the phase or line voltages. An inequality in the phase voltage produces an inequality in the line voltages. These phase or line voltages can differ in magnitude or phase or both. There are several causes of voltage unbalance on the power system. The major cause of unbalanced voltages is a disproportionate share of the single-phase loads on the three-phase networks (unbalanced loads). This can occur directly on the distribution system but also in the manufacturing plants with a non-uniform spread of single-phase loads within the plant. The other causes are; open circuit in one of the phases, often caused by a blown fuse, incomplete or no transposition of transmission lines, using different cable sizes causing different voltages in three-phase systems etc. [1 - 15].

A considerable amount of work has been done concerning induction motor operation under unbalanced voltages. This work can be found since the 1950s in the American Institute of Electrical Engineers (AIEE) Transactions, presently known as the Institute of Electrical and Electronics Engineers (IEEE). The National Electrical Manufacturers Association (NEMA) has also done research on motors operating under unbalance supplies, that is, they defined voltage unbalance and produced a derating curve to be used in industry to protect motors from unbalanced voltages. The International Electro-technical Commission (IEC) has another definition of voltage unbalance, which differs from that of NEMA. The difference between the two definitions needs to be addressed.

In practice, induction motors experience a combination of overvoltages or undervoltages with unbalanced voltages at the motor terminals. The tolerable level for voltage unbalance on the South African three-phase networks is 2%, and may be up to 3% in the rural areas [31]. During peak hours, some customers with three-phase motors could experience the minimum voltages guaranteed by

the utility, with a combination of voltage unbalance. In order to minimise the costs, modern motors are designed to make the best use of materials and sized more closely to their nameplate ratings than older motors. As a consequence, their ability to operate under abnormal conditions is reduced compared to the older, over-designed motors. The performance of the motor under these conditions needs to be investigated. The motor life span is of great concern as it has an effect on the productivity of the company. Being able to estimate the motor life under these conditions will guide the user to run the plant efficiently.

1.3 LITERATURE SURVEY ON THE EFFECTS OF VOLTAGE UNBALANCE ON INDUCTION MACHINES

1.3.1 Symmetrical Components

In 1918, C.L. Fortescue developed a powerful technique for analyzing three-phase unbalanced systems. This method decouples a three-phase unbalanced system into three balanced sequence networks. These three sequence networks can be analyzed separately and the overall effect can be found by superposition. The three sets of sequence components are:

- Positive sequence components. Three phasors in the normal a-b-c sequence with equal magnitudes and 120° phase displacement.
- Negative sequence components. Three phasors in the reversed a-c-b sequence with equal magnitudes and 120° phase displacement.
- Zero sequence components. Three phasors with equal magnitudes and with zero phase displacement.

Induction motors are typically connected in delta or ungrounded star and as a result, the line currents have no zero sequence component, except during a fault [3,10,12,16,27]. In addition, the sum of the line voltages is zero because these

voltages form a close triangle in the absence of a fault. Since the zero sequence component is eliminated, the line voltages are resolved into a positive sequence voltage component V_p , and a negative sequence voltage component V_n . The conversion is shown below:

$$V_p = \frac{V_{ab} + a \cdot V_{bc} + a^2 \cdot V_{ca}}{3}, \quad (1.1)$$

$$V_n = \frac{V_{ab} + a^2 \cdot V_{bc} + a \cdot V_{ca}}{3}, \quad (1.2)$$

where V_{ab} , V_{bc} and V_{ca} are line voltages,

$$a = 1 \angle 120^\circ \text{ and } a^2 = 1 \angle 240^\circ$$

Each sequence component has its own equivalent circuit as shown in figures 1.1 and 1.2. The behaviour of an induction machine to the positive sequence voltage is the same as for the normal balanced operation. The negative sequence voltage produces negative sequence currents in the motor, which create magnetic fields that oppose the direction of the fields due to the positive sequence currents. The motor behaves as a combination of two machines, one with a phase voltage V_p and slip s , the other with V_n and slip $(2 - s)$.

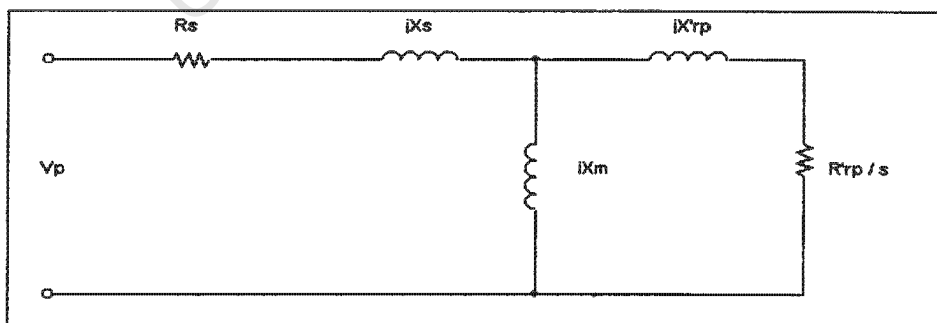


Figure 1.1: Positive sequence equivalent circuit

Where R_s = stator resistance and X_s = stator reactance

R'_{rp} = positive sequence rotor resistance

X'_{rp} = positive sequence rotor reactance

V_p = positive sequence voltage

X_m = magnetizing reactance and s = slip

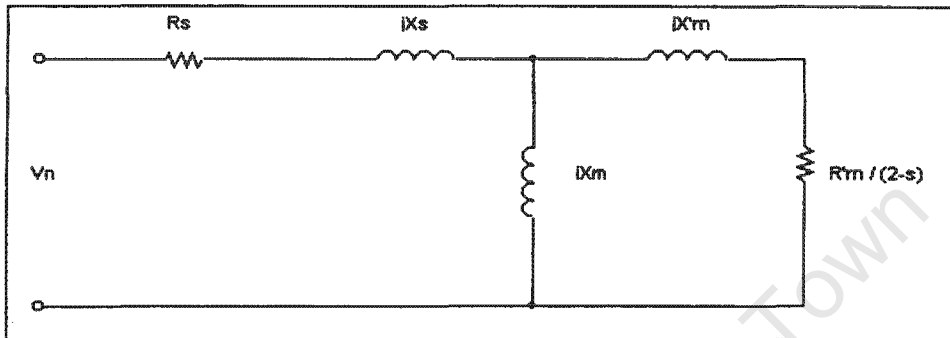


Figure 1.2: Negative sequence equivalent circuit

Where R'_m = negative sequence rotor resistance

X'_m = negative sequence rotor reactance

V_n = negative sequence voltage

The positive and negative equivalent circuits are used when analysing the performance on induction machines operating from unbalanced supplies. The most critical effects of voltage unbalance on motors are mentioned below.

*1.3.2 Effects of Voltage Unbalance on the Induction Machine

- The stator currents are greatly unbalanced, much more so than the voltage unbalance. Current unbalance in an order of six to ten times the voltage unbalance can occur due to the negative sequence impedance of the motor being many times smaller than the positive sequence impedance. This increased current adds to the resistive losses and gives rise to serious

overheating and a reduction in insulation life, unless the motor is derated [1,10,13].

- The rotor losses increase at a faster rate than the stator losses as the voltages become more unbalanced. The excessive rotor temperature weakens the rotor structure and bearings as heat is more difficult to remove from the rotor than from the stator [12].
- The mechanical power and torque are reduced by the presence of the negative sequence currents. The torque reduction is a problem when full load is demanded because the motor will be forced to operate at higher than rated slip to meet the torque requirements. As a result, the motor losses and temperature will increase [2,9,10,16]. During start up, the motor can take a longer time to run up to full load, due to the reduction in the torque-speed envelope, which will increase the temperature rise, which in turn reduces the insulation life.
- Mechanical stresses are increased due to the fluctuating power and the backward rotating field. Noise and vibration levels are increased by the presence of the negative sequence components. Vibrations can cause damage to bearings, insulation and interconnected mechanical equipment [2,10].
- Voltage unbalance causes additional load to utilities and additional charges to customers. This is because of the decrease in motor efficiency, which increases the demanded input power to drive the motor to meet the required load [11]. This causes additional electricity and maintenance costs to the industry, reducing their competitiveness and thus ultimately affecting the health of the power company.

- The rotor is also affected by its impedance, which is frequency dependent. This phenomenon is known as the “skin effect”. High frequency causes the rotor current to concentrate on the surface of the rotor conductors, thus increasing the effective rotor resistance and decreasing the effective rotor leakage reactance. The rotor resistive losses will increase due to the increase of the effective rotor resistance [1,10,13].

The rotor type has an effect on the negative sequence impedance. The double-cage rotor, used for high starting torque at moderate currents, has higher resistance than single-cage rotors at startup. Williams showed the difference in additional losses for two types of rotors [1]. He concluded that additional losses due to voltage unbalance are larger for motors with multiple-cage rotors.

The effects of voltage unbalance can be summarised by stating that voltage unbalance causes a negative sequence component, which causes additional motor losses and reduced torque.*These additional losses cause an increase in temperature rise above rated, which reduces motor life.

This review has suggested that there is loss of motor life due to voltage unbalance. How much life is reduced will depend on the magnitude of voltage unbalance. Little work has been done on estimating motor life when operated under unbalanced voltages. No work has been done on motor life when the motor is supplied with a combination of over or undervoltage with unbalance. This project will provide an estimation of motor life under unbalance alone and also with a combination over and undervoltages.

1.4 LITERATURE SURVEY ON MOTOR LIFE

The lifetime of a motor is defined as the period of time from the completion of its fabrication to the time where its required performance can no longer be achieved. Depending on the specific load applications and environmental conditions, the life of motors can have a span of 10 to 40 years [17]. For long-term applications, the estimation of lifetime expectancies of a motor is determined by the user since the manufacturers rarely predict the lifetime beyond the warranty periods.

* Lifetime expectancy of the motor is determined by estimating the insulation life. The other causes of motor failure such as environmental and mechanical effects are considered random and are influenced by the load configuration. *The relationship between temperature and time determines the insulation life span. The concept of the 10°C rule introduced by Montsinger stated that the insulation thermal life is halved for each increase of 10 °C at the operating temperature. An equation was developed using Arrhenius law to estimate the insulation life [18]. This equation modifies Montsinger's rule to be more accurate and is expressed as follows:

$$L_x = L_{100} \cdot 2 \cdot e^{(T_c - T_x)/HIC} \quad \text{in (yrs, hrs, min, etc),} \quad (1.3)$$

where L_x = Percent lifetime at temperature, T_x (°C)

L_{100} = Percent lifetime at rated temperature, T_c (°C)

T_x = Hot-spot temperature for insulation class, (°C)

T_c = Total allowable temperature for insulation class, (°C)

HIC = Halving interval, (°C) (14, 11, 9.3, 8 and 10 for class A, B, F, H and H' respectively)

The percent lifetime of motor, L_x , is stated in terms of percent lifetime of the rated life, L_{100} . The Arrhenius equation can be used to estimate the insulation life of the

motor in the presence of unbalanced voltages. What needs to be determined is the additional heating due to unbalanced currents. For calculation purposes, the motor temperature rise can be obtained from an accurate thermal model.

1.5 LITERATURE SURVEY ON THERMAL MODELS

Various researchers have developed both transient and steady state thermal models to estimate the induction motor temperature under balanced conditions. Very few of these models accommodate unbalance conditions. Most of the thermal models are complex and require the machine physical dimensions when determining the model parameters. Equation 1.4 is a general equation which relates the sources of heat $[P]$ and the temperature rise $[\theta]$ in the time domain for the stator as well as the rotor. This equation is used in many thermal models [21 – 25].

$$\frac{d[\theta]}{dt} = [C]^{-1} * ([P] - [G][\theta]), \quad (1.4)$$

where $[G]$ = Thermal conductance matrix

$[C]$ = Thermal capacitance matrix

Simple tests can be performed to determine these parameters, which do not require machine dimension data, which is generally not available. A thermal model will be developed based on simple but practical tests. The model is required to work under balanced, unbalanced, over and undervoltages at different load conditions. This thermal model will help to estimate the motor temperature rise at any given time without making direct measurements.* From the temperature rise, motor life can be estimated.

1.6 LITERATURE SURVEY ON RELEVANT PAPERS

The paper that is most relevant to this project presents a method for analysing the thermal behaviour of a three-phase squirrel cage induction motor operating under balanced and unbalanced supplies [21]. The calculation of the thermal behaviour consists of electrical, mechanical and thermal models, which are interconnected. A set of equations, in the time domain, representing the models were defined and implemented in a simulator known as SABER. This simulator allows transient and steady state calculations. The data used in the models were based on measurements and design data.

The thermal model was developed separately for the stator and rotor. The model works under both transient and steady state conditions. Determining the model parameters, $[G]$ and $[C]$, using simple techniques is a challenge as most of the thermal models use complex methods. Oliveria *at al.* stated that thermal conductance data, $[G]$, can be found from catalogues, manufacturers or design data [21]. He obtained the thermal capacitance data, $[C]$, from a general equation,

$$C = mc \text{ [Ws/}^\circ\text{C]}, \quad (1.5)$$

where c = specific heat of insulation $[\text{Ws/}^\circ\text{C kg}]$,

m = winding/core mass $[\text{kg}]$.

Equation 1.5 requires the physical dimensions of the winding, core masses and also the insulation characteristics.

The heat sources $[P]$ considered from the electrical model were the I^2R losses in the stator and rotor, core loss, mechanical losses and stray load losses. The

change in the rotor impedance with frequency was also considered. The core loss was included in the equivalent impedance of the electrical model. The mechanical losses (friction and windage) were included in the motor shaft output. The stray load loss was assumed to be 0.5% of the rated losses and was also included in the motor shaft output. This covers all the losses in an induction machine.

Oliveria simulated four cases with different voltage unbalance and harmonic distortions in order to study the thermal behaviour of the induction motor. Due to the increase of stator winding temperature above rated conditions, the reduction in motor insulation life was estimated using equation 1.6, which is essentially the same as equation 1.3.

$$p_1 = p_2 * \exp\left[\left(-\frac{E}{K}\right) * \frac{\Delta\theta}{\theta_2 (\theta_2 + \Delta\theta)}\right] \quad (1.6)$$

where p_1 = reduction of motor life

p_2 = useful life of the motor under rated conditions

$\Delta\theta$ = temperature rise in relation with θ_2 °C

θ_2 = absolute temperature

E = activation energy

K = boltzman constant

* The simple way to restore motor life under unbalanced voltage is to derate the motor. Thus the motor will operate below its rated conditions generating a lower output. Having an estimate of how much life is lost will guide the user to apply the correct derating. The next section addresses the literature survey on motor derating.

1.7 LITERATURE SURVEY ON MOTOR DERATING

NEMA has developed a derating curve for various induction machines as shown in figure 1.3. It can be seen from the graph that a motor should start to be derated above 1% voltage unbalance. NEMA does not recommend the operation of motors above 5% voltage unbalance due to serious overheating. The derating curve in figure 1.3 was developed from the following equation,

$$1 + \frac{2(\text{percent unbalance})^2}{100} = \left(\frac{\text{percent load}}{100} \right)^{-1.7} \quad (1.7)$$

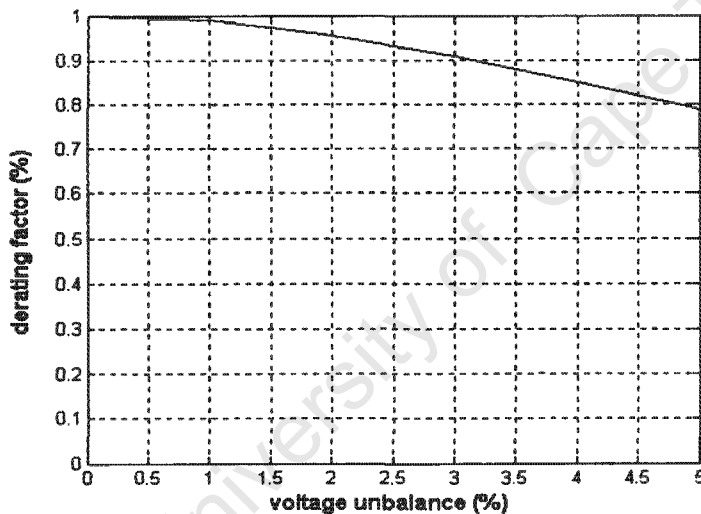


Figure 1.3: NEMA derating curve

It is evident on the graph that overvoltages and undervoltages are not included. NEMA assumes that the average voltage used in its definition of voltage unbalance is always equal to the rated voltage. In practice, motors experience a combination of over or undervoltages with unbalanced voltages. In order to ensure correct motor derating, the NEMA curve has to be extended to include these conditions.

1.8 SUMMARY AND DISCUSSION OF THE PROJECT

The relevant literature surveys on the effects of voltage unbalance on induction motors, motor life, thermal models and motor derating were discussed. These surveys form the basic foundation of the undertaken research project by identifying the work that needs to be done in this area.

The most common and serious effect of unbalanced voltages is overheating, which reduces motor life. Only one paper reviewed attempts to do this, but the authors do not consider the effects of overvoltages and undervoltages in the presence of unbalanced voltages [1]. They also developed a snapshot of increased temperature rise and hence a reduction in life, but they have not done any work on the appropriate derating to restore motor life.

Work has been done to develop thermal models and equations for estimating insulation life. However, very few of these models accommodate unbalanced voltages under different load conditions. The thermal parameters were determined from design data.

1.9 CONTRIBUTION OF THIS THESIS

The objectives of this project are:

- To identify, analyse and compare the definitions of voltage unbalance.
- To develop techniques to determine thermal parameters from tests rather than from motor design data, which is almost never available at industrial plants.

- To estimate motor life of a three-phase induction motor when supplied with unbalanced voltages in the presence of overvoltages or undervoltages.
- To include overvoltages and undervoltages with unbalanced voltages on the NEMA derating to restore motor life.

University of Cape Town

Chapter 2

2. DEFINITIONS OF VOLTAGE UNBALANCE

2.1 INTRODUCTION

This chapter addresses the definitions of voltage unbalance developed by NEMA, IEEE and IEC. These definitions are used when studying the effects of voltage unbalance on three-phase induction machines. An analysis was done in order to understand the implications of using these definitions of voltage unbalance, as it pertains to the South African power system. This will help the user to understand the difference in these definitions and their impact on electrical equipment.

2.2 DEFINITIONS OF VOLTAGE UNBALANCE

2.2.1 NEMA Definition

The NEMA definition of voltage unbalance, also known as the line voltage unbalance rate (LVUR) [11,26,28 - 30], is given by:

$$\% \text{ LVUR} = \frac{\text{maximum voltage deviation from the average line voltage}}{\text{average line voltage}} \cdot 100. \quad (2.1)$$

The NEMA definition assumes that the average voltage is always equal to the rated value, which is 380 V for the South African three-phase systems. This definition works with magnitudes only, phase angles are not included.

2.2.2 IEEE Definition

The IEEE definition of voltage unbalance, also known as the phase voltage unbalance rate (PVUR) [11], is given by:

$$\% \text{ PVUR} = \frac{\text{maximum voltage deviation from the average phase voltage}}{\text{average phase voltage}} \cdot 100 \quad (2.2)$$

The IEEE uses the same definition of voltage unbalance as NEMA, the only difference being that the IEEE uses phase voltages rather than line-to-line voltages. Here again, phase angle information is lost since only magnitudes are considered.

2.2.3 IEC Definition

The IEC or the 'true' definition of voltage unbalance is defined as the ratio of the negative sequence voltage component to the positive sequence voltage component [11,28,31]. The percentage voltage unbalance factor (% VUF) or the true definition is given by:

$$\% \text{ VUF} = \frac{\text{negative sequence voltage component}}{\text{positive sequence voltage component}} \cdot 100 \quad (2.3)$$

The positive and negative sequence voltage components are obtained by resolving three-phase unbalanced phase or line voltages into two symmetrical components of the phase or line voltages. The positive and negative sequence components are calculated using equations 1.1 and 1.2.

The true definition involves both magnitude and angles when calculating the positive and negative sequence voltage components. An alternative formula that

avoids the use of complex algebra and gives the same results as the true definition is given by:

$$\% \text{ voltage unbalance} = \sqrt{\frac{1 - \sqrt{3 - 6\beta}}{1 + \sqrt{3 - 6\beta}}} \cdot 100 \quad (2.4)$$

$$\text{where } \beta = \frac{V^4_{ab} + V^4_{bc} + V^4_{ca}}{(V^2_{ab} + V^2_{bc} + V^2_{ca})^2}$$

This formula will be referred as 'beta' formula.

2.2.4 Approximation Formula

Another equation that gives a good approximation of the true definition is given by.

$$\% \text{ voltage unbalance} = \frac{82 \cdot \sqrt{V^2_{abe} + V^2_{bce} + V^2_{cae}}}{\text{average line voltage}} \quad (2.5)$$

where V_{abe} = difference between the line voltage V_{ab} and the average line voltage, etc.

2.3 ANALYSIS OF THE DEFINITIONS OF VOLTAGE UNBALANCE

Suppose three unbalanced line-to-line voltages $V_{ab} = 456 \angle 0^\circ$, $V_{bc} = 310 \angle 234^\circ$ and $V_{ca} = 374 \angle 137^\circ$ are applied to an induction motor. The average value will be $(456 + 310 + 374)/3 = 380$ V and the maximum deviation from average value is $(456 - 380) = 76$ V. Therefore, the NEMA definition of voltage unbalance will be $100(76/380) = 20$ %.

The positive sequence voltage $V_p = 373.8 \angle 4.19^\circ$ and the negative sequence voltage $V_n = 86.7 \angle -18.4^\circ$. The true definition of % voltage unbalance will be $100(86.7/374.8) = 23.1\%$. Applying the same set of voltages to the approximation formula, results in $V_{abe} = (456 - 380) = 76$ V, $V_{bce} = (380 - 310) = 70$ V, and $V_{cae} = (380 - 374) = 6$ V, therefore % voltage unbalance will be $82(103.5/380) = 22.3\%$. This value is close to the true definition of voltage unbalance. The motor will respond to the true value of voltage unbalance, but NEMA will be assuming 20% unbalance for the same set of voltages.

In order to understand the implications of using these definitions of voltage unbalance, the following analysis was done.

Suppose three unbalanced line voltages are defined as follows:

$$\bar{E}_{ab} = E_{ab} \angle 0^\circ, \quad \bar{E}_{bc} = E_{bc} \angle \theta_{bc} \quad \text{and} \quad \bar{E}_{ca} = E_{ca} \angle \theta_{ca}$$

For a given percentage of voltage unbalance based on the NEMA definition, say 5% and assuming an average voltage of 380 V and naming the line voltage with the largest deviation from the average, E_{ab} . Then the following calculations are made:

$$\% \text{ LVUR} = \frac{E_{ab} - 380}{380} = 0.05 \tag{2.6}$$

$$E_{ab} - 380 = 0.05 \cdot 380 = 19 \quad \therefore E_{ab} = 399 \text{ V}$$

$$\text{The average voltage} = \frac{E_{ab} + E_{bc} + E_{ca}}{3} = 380 \text{ V}$$

$$\therefore E_{bc} + E_{ca} = 741 \text{ V} \quad \text{and} \quad E_{ca} = 741 - E_{bc}$$

E_{bc} and E_{ca} can be written as $|E_{bc} - 380| < 19$ and $|E_{ca} - 380| < 19$ respectively. This is so because E_a has the largest deviation from average. Hence,

$$361 < E_{bc} < 380 \quad \text{and} \quad 361 < E_{ca} < 380$$

The vector sum of the line voltages $\bar{E}_{ab} + \bar{E}_{bc} + \bar{E}_{ca} = 0$, since the zero sequence voltage must be zero in the absence of a fault. This equation can be resolved as follows:

$$E_{ab} \angle 0^\circ + E_{bc} \angle \theta_{bc} + E_{ca} \angle \theta_{ca} = 0 \quad (2.7)$$

$$399 + E_{bc} \cdot \cos \theta_{bc} + j E_{bc} \cdot \sin \theta_{bc} + (741 - E_{bc}) \cdot \cos \theta_{ca} + j (741 - E_{bc}) \cdot \sin \theta_{ca} = 0$$

So for a given E_{bc} , angle θ_{bc} and angle θ_{ca} can be found from the above equation by separating it into two parts, real and imaginary, and solving the two equations.

From the above calculations, the true definition of voltage unbalance will be:

$$\% \text{ VUF} = \frac{399 \angle 0^\circ + a^2 \cdot E_{bc} \angle \theta_{bc} + a \cdot (741 - E_{bc}) \angle \theta_{ca}}{399 \angle 0^\circ + a \cdot E_{bc} \angle \theta_{bc} + a^2 \cdot (741 - E_{bc}) \angle \theta_{ca}} \cdot 100 \quad (2.8)$$

where $a = 1 \angle 120^\circ$ and $a^2 = 1 \angle 240^\circ$

The approximation formula will be:

$$\% \text{ unbalance} = \frac{82 \cdot \sqrt{(399 - 380)^2 + (E_b - 380)^2 + ((741 - E_b) - 380)^2}}{380} \quad (2.9)$$

From this analysis, it has been found that for a given value of % unbalance, based on the NEMA definition, there is range of % unbalance, based on the true definition, beta formula and the approximation formula. This is shown in figure 2.1 for 2%, 5%, 10% and 20% based on NEMA definition of voltage unbalance.

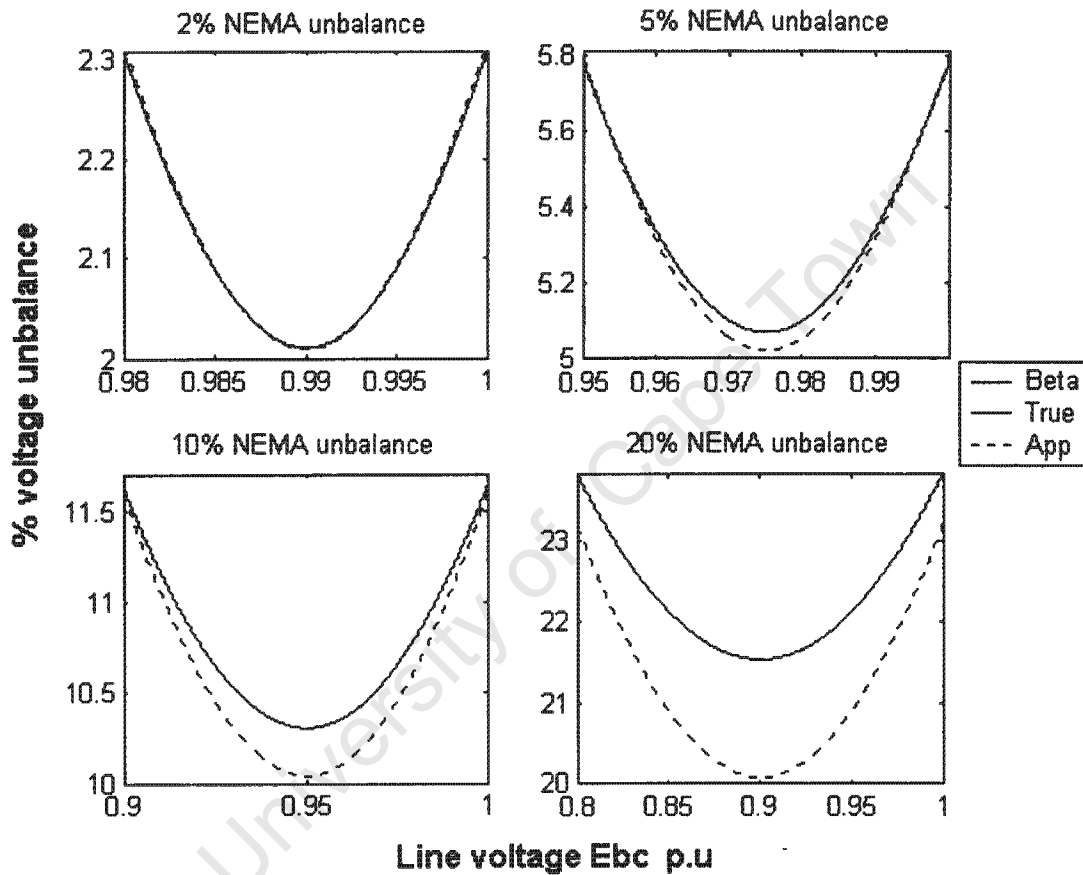


Figure 2.1: Relationship of the definitions of voltage unbalance

Figure 2.1 shows that for 2% and 5% NEMA unbalance, the true definition and the approximation formula agree very closely. As voltage unbalance increases above 5%, based on NEMA, the approximation formula starts to deviate from the true definition. The true definition and the beta formula have the same % unbalance values.

Table 2.1 shows the range of the true definition and the approximate formula for 2%, 5%, 10% and 20% NEMA unbalance. It is clear from the table that the deviation range of the true definition and the approximation formula from NEMA unbalance are almost the same. The focus will now be between the NEMA definition and the true definition of voltage unbalance.

Table 2.1: Range of voltage unbalance

NEMA	True definition	Approximation formula
%	%	%
2	2 – 2.3	2 - 2.3
5	5 – 5.8	5 - 5.8
10	10.3 - 11.6	10 - 11.6
20	21 - 23.8	20 - 23.2

Below 5% unbalance, based on NEMA unbalance, the maximum difference between the NEMA definition and the true definition is 0.8%. Above that, say 20%, the difference can be as high as 3.8%. The NEMA definition and the true definition differ substantially when the voltage unbalance is extremely high as shown in the example and in figure 2.1.

The above analysis is based on line voltage magnitudes. E_{ab} was kept constant, E_{bc} and E_{ca} were varied such that the average line voltage remained at 380V. Figure 2.1 shows how E_{bc} varies with % voltage unbalance. Since both magnitudes and angles are unbalanced, it is important to analyze the angles in order to determine their relationship with the definitions of voltage unbalance. This was done by choosing angle θ_{bc} instead of the line voltage magnitude E_{bc} such that equations 2.6 to 2.9 are satisfied.

Figure 2.2 shows the relationship between the angle θ_{bc} and the definitions of voltage unbalance. The x-axis represents the angle deviation from the balanced angle $\theta_{bc} = 240^\circ$. For example, at 5% NEMA unbalance, the deviation from 240° is from 0.25° to 4.85° and therefore the true range of angles will be $(240 - 0.25)$ to $(240 - 4.85) = 239.75^\circ$ to 235.15° . The deviation range for θ_{ca} from a balance angle of 120° can also be shown in the same way. Note that the relationship between the definitions of voltage unbalance in figure 2.2 is the same as in figure 2.1.

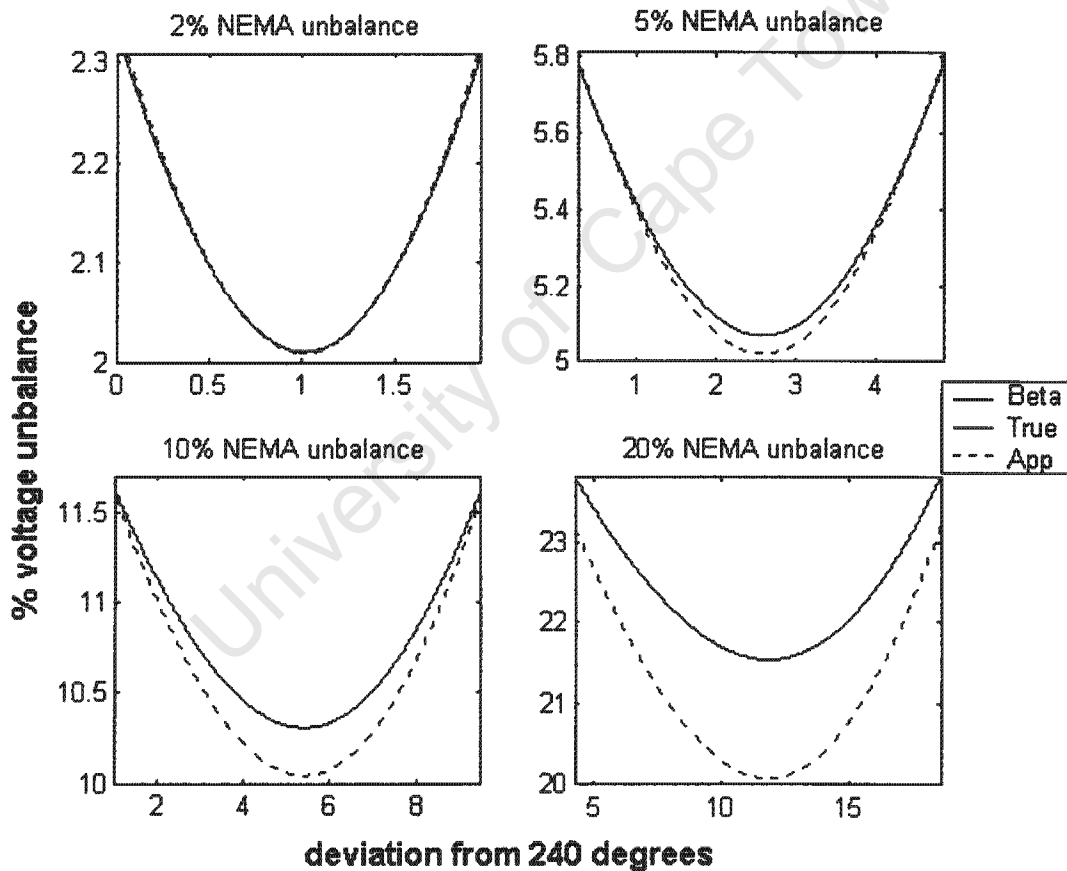


Figure 2.2: Relationship of the definitions of voltage unbalance with angle variation

When studying the effects of voltage unbalance on induction machines, the positive and negative sequence equivalent circuits are often used. Hence the true definition is used. In this project, the true definition of voltage unbalance will be used when developing new derating curves based on the NEMA derating curve when a motor is supplied with a combination of over or undervoltages with unbalanced voltages. The question that needs to be answered is to determine whether the use of the true definition on the NEMA curve is significant or not when derating the machine.

2.4 COMPARISON OF NEMA DEFINITION AND TRUE DEFINITION OF VOLTAGE UNBALANCE

The NEMA derating curve is limited to 5% unbalance and operating a motor above 5% unbalance is not recommended. Figure 2.3 shows the relationship between the NEMA definition and the true definition of voltage unbalance up to 5% unbalance. For one value of unbalance based on NEMA, there is a range of values from the true definition. The maximum deviation between the NEMA and the true definitions below 5% unbalance is 0.8%.

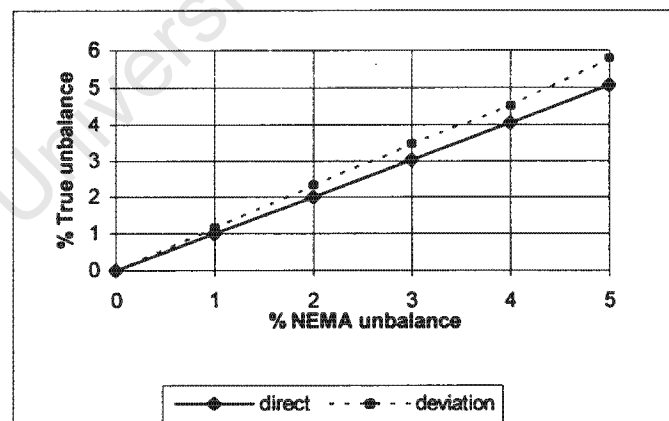


Figure 2.3: Relationship between the NEMA and the true definitions of voltage unbalance

The purpose of this analysis is to determine whether the difference between the two definitions is significant or not. This was done by looking into the motor losses, efficiency and temperature rise at 5% and 5.8% voltage unbalance

A 3kW, 50 Hz, induction motor was modelled using the positive and negative sequence circuits. Appendices A and B show the motor ratings and parameters respectively. The motor parameters were checked by comparing the measured input currents, total losses and efficiency with the calculated values at full load.

The total losses of the motor at full load with 0% unbalance were 687 W. At 5 % unbalance, based on true definition (same as NEMA % unbalance), the calculated total losses were 781 W. With 5.8% unbalance using the true definition, the losses were 793 W at each extreme end of the definition, an increase of 12 W. The losses changed by 1.5% from 5% - 5.8% unbalance. The negative sequence voltage component is increased from 5% to 5.8% of the average voltage by 0.8%. The efficiency of the motor at 5% unbalance was 79.9% and the efficiency at 5.8% unbalance was 79.5%, a decrease of 0.4%. The temperature at 5% unbalance was 113° and at 5.8% unbalance was 114°, an increase of 1°.

The negative voltage component, total losses, efficiency and temperature from 5% – 5.8% unbalance do not change by significant magnitudes, therefore, one can use the true definition of voltage unbalance on the NEMA derating curve. However, it is important to know that these differences exist.

2.5 CONCLUSIONS

This chapter has addressed the relationship between the definitions of voltage unbalance. An analysis was done to show how these definitions are related. It was found that for a given NEMA unbalance, there is a range of unbalance based on the true definition, beta formula and the approximation formula. At 5% unbalance, based on NEMA unbalance, the maximum deviation between the NEMA definition and the true definition is 0.8%. The difference is high for extreme values of % unbalance based on the NEMA definition.

The positive and negative sequence circuits were used to test whether the use of the true definition on the NEMA derating curve is significant when derating the machine or not. The motor total losses, efficiency and temperature rise were calculated at 5% and 5.8% unbalance. Up to 5% unbalance, there is not much of a difference between the two definitions. It was concluded that the true definition of voltage unbalance can be used on the NEMA derating curve.

Chapter 3

3. ELECTRICAL AND THERMAL MODELS

3.1 INTRODUCTION

This chapter addresses the development of electrical and thermal models of a three-phase squirrel cage induction machine. The purpose of developing an electrical model is to be able to simulate the motor's electrical performance characteristics. The output of the electrical model feeds the thermal model to predict the motor temperature rise.

The interaction between the electrical model and the thermal model is particularly important when simulating the motor's performance when operating under unbalanced voltages, in combination with overvoltages and undervoltages. This will also improve motor protection. The flow chart in figure 3.1 shows the connection of the electrical and thermal models to predict motor temperature. The main idea in this chapter is to identify the correct model, find its parameters and determine the motor performance using the model.

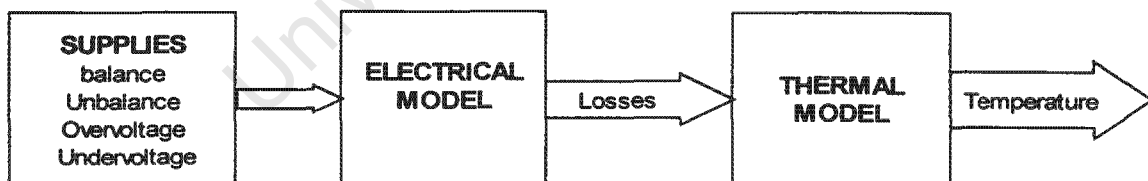


Figure 3.1: Electrical and thermal models flow-chart

3.2 ELECTRICAL MODEL OF AN INDUCTION MACHINE

Induction motor equivalent circuits are found in many textbooks [16,28,32,33]. Since unbalanced voltages are to be simulated using symmetrical components, both positive and negative sequence equivalent circuits will be used.

3.2.1 Positive and Negative Sequence Equivalent Circuits

Figures 3.2 and 3.3 show the positive and the negative sequence equivalent circuits. The behaviour of an induction machine to the positive sequence voltage is the same as for normal balanced operation. The negative sequence voltage produces negative sequence currents in the motor, which create magnetic fields that oppose the direction of the fields due to the positive sequence currents. The motor behaves as a combination of two machines, one with voltage V_p and slip s , and another machine with voltage V_n and slip of $(2 - s)$.

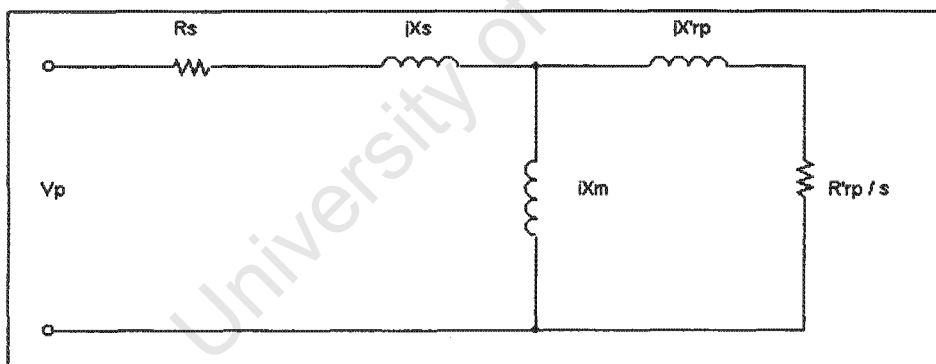


Figure 3.2: Positive sequence equivalent circuit

Where R_s = stator resistance and X_s = stator reactance

R'_{rp} = positive sequence rotor resistance

X'_{rp} = positive sequence rotor reactance

V_p = positive sequence phase voltage

X_m = magnetizing reactance and s = slip

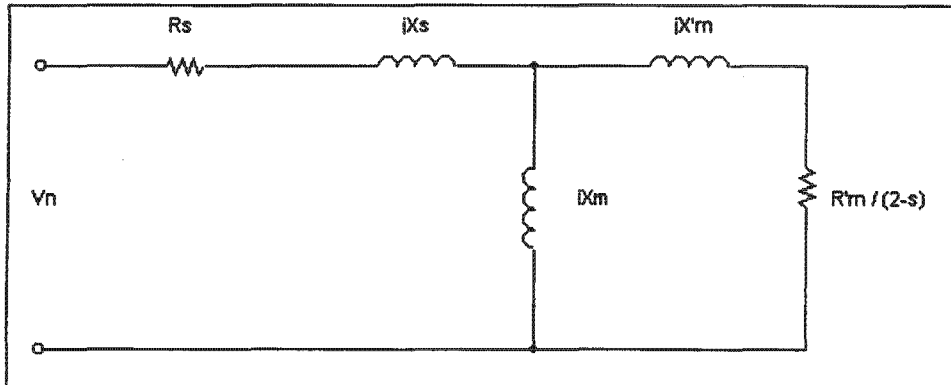


Figure 3.3: Negative sequence equivalent circuit

Where R'_m = negative sequence rotor resistance

X'_m = negative sequence rotor reactance

V_n = negative sequence phase voltage

3.2.2 Equivalent Circuit Parameter Determination

The parameters of the positive sequence circuit in figure 3.2 were obtained from no-load and short circuit tests. The negative sequence rotor resistance and reactance are at a higher rotor frequency (two times the supply frequency) and were obtained using the method in [23]. The negative sequence stator resistance, leakage reactance and magnetizing reactance are the same as for the positive sequence circuit because they are at the same frequency. Appendix B shows the parameters of a 3 kW induction motor.

3.2.3 Motor Performance Characteristics

Stator Winding Loss

The total stator winding loss was obtained by multiplying the square of the positive and negative sequence input currents each by the stator resistance. The input currents were calculated using the motor equivalent circuit with the respective terminal voltages and input impedance. To determine the winding loss for each phase under unbalance, the currents were transformed back into normal *rms* currents I_a , I_b and I_c .

Core Loss

The induction motor was run on no-load. The core loss was obtained by subtracting the stator winding loss, friction and windage loss from the no-load input power. The core losses were determined for three cases. Case 1: The core loss test was done at rated average voltage with 0 to 5% unbalanced voltage. Case 2: The motor was supplied with 10% overvoltage with 0 to 5% unbalance. Case 3 was done with 10% undervoltage with the same range of unbalance. Figure 3.4 shows how the core loss increases with voltage unbalance when the motor is supplied with rated average voltage, 10% overvoltage and 10% undervoltage respectively.

Figure 3.5 shows the core loss as a function of average voltage from 90% – 110%. The core loss can be obtained for any average voltage value between 90% and 110% with 0% to 5% voltage unbalance. This is useful when determining the motor performance when operating at average voltages other than 90%, 100% and 110%.

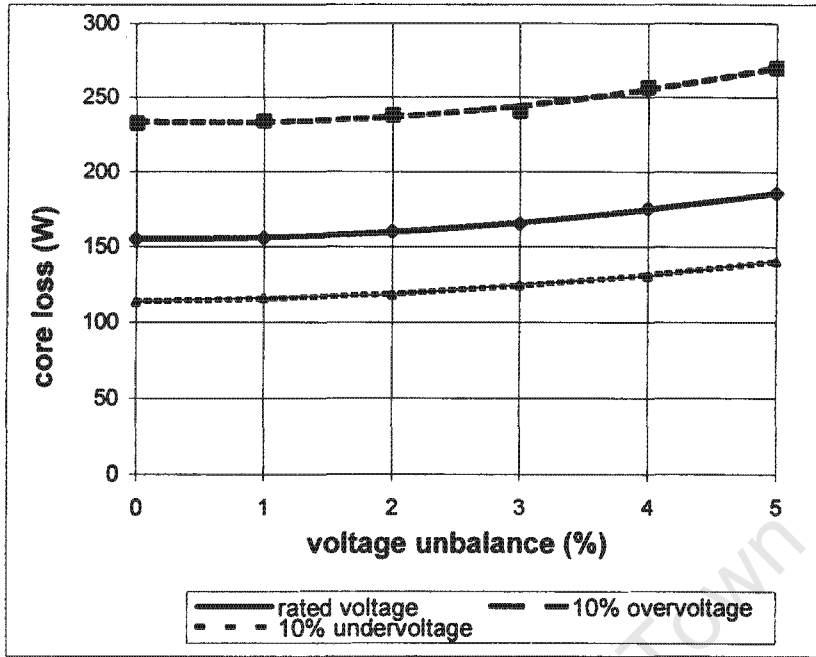


Figure 3.4: Core loss at rated, 10% overvoltage and undervoltage with unbalanced voltages

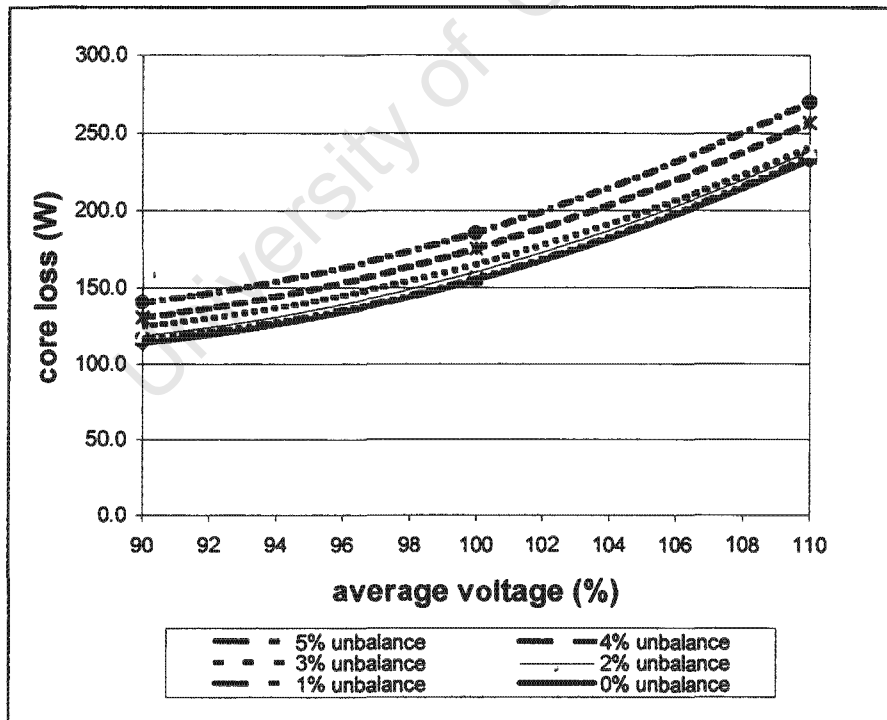


Figure 3.5: Core loss from 90% -110% average voltages with unbalanced voltages

Developed Power and Torque

The total mechanical power due to the positive and negative sequence currents is given by:

$$P_m = I'^2_{rp} \cdot R'_{rp} \cdot \left(\frac{1-s}{s} \right) - I'^2_{m} \cdot R'_{m} \cdot \left(\frac{1-s}{2-s} \right) \text{ watts, per phase,} \quad (3.1)$$

where I'^2_{rp} and I'^2_{m} are the positive and negative sequence rotor currents respectively.

The total torque will be:

$$T_m = I'^2_{rp} \cdot R'_{rp} \cdot \left(\frac{1}{s \cdot W_0} \right) - I'^2_{m} \cdot R'_{m} \cdot \left[\frac{1}{(2-s) \cdot W_0} \right] \text{ N.m, per phase,} \quad (3.2)$$

where W_0 is the synchronous speed in radians per second.

The positive and negative sequence rotor currents can be obtained from equations 3.3 and 3.4 provided the slip and motor parameters are known.

$$I'_{rp} = \frac{E_p}{\sqrt{[R_s + (R'_{rp}/s)]^2 + (X_s + X'_{rp})^2}} \text{ A, per phase,} \quad (3.3)$$

$$I'_{m} = \frac{E_n}{\sqrt{[R_s + (R'_{m}/(2-s))]^2 + (X_s + X'_{m})^2}} \text{ A, per phase,} \quad (3.4)$$

where E_p and E_n are positive and negative sequence airgap voltages.

Equations 3.1 and 3.2 show that the total mechanical power and torque are reduced by the presence of negative sequence currents. Using the positive and negative sequence equivalent circuits, core loss curves and the above equations, the motor characteristics can be determined when the motor is supplied a combination of over or undervoltages with unbalanced voltages.

3.3 THERMAL MODEL OF AN INDUCTION MACHINE

Both transient and steady state thermal models are being developed to estimate the induction motor temperature. Most of these thermal models are complex and require the machine physical dimensions when determining the model parameters. Simple tests can be performed to determine these parameters rather than using machine dimension data, which is generally not available.

A simple thermal model that estimates both transient and steady state temperatures of a three-phase squirrel cage induction motor was developed. The assumption made was that the rotor heat does not flow through the stator to the ambient but via the shaft to the ambient [21, 23, 24]. This was also verified experimentally. This uncouples the stator and rotor thermal circuits. The main focus is on the stator side of the motor because the stator winding temperature is of interest when estimating motor life and derating. This thermal model should be able to estimate the temperature rise caused by both balanced and unbalanced voltages at different load conditions.

3.3.1 Thermal Model Circuits

Figures 3.6 and 3.7 show stator and rotor thermal model circuits of an induction motor respectively [21]. These models are made up of heat sources, thermal capacitance and thermal conductance. Since the stator model is supposed to include voltage unbalance, all three phases are shown in figure 3.6. Each phase

is represented by a heat source and three conductances, two linking it to the other phases and one to the core.

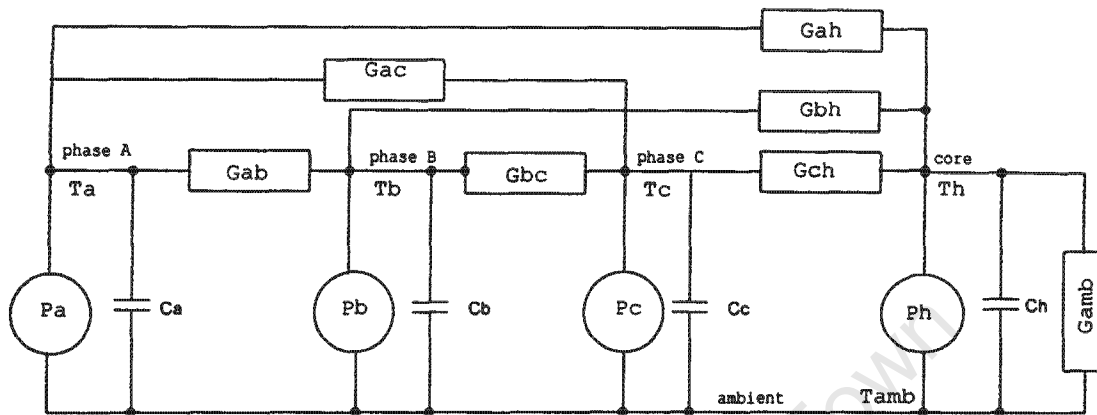


Figure 3.6: Stator thermal model circuit

where P_a, P_b, P_c = stator copper loss of phase A, B and C respectively, (W)

P_h = stator core loss

G_{ab}, G_{bc}, G_{ac} = thermal conductance between two phases, (W/°C)

G_{ah}, G_{bh}, G_{ch} = thermal conductance between phase and core

G_{amb} = thermal conductance between core and ambient

T_a, T_b, T_c = phase A, B, C stator winding temperature, respectively,

T_h, T_{amb} = core and ambient temperature, (°C)

C_a, C_b, C_c, C_h = thermal capacitance, (Ws/°C)

The rotor thermal model consists of a heat source from the bars, thermal conductance to the core and heat source as result of core losses.

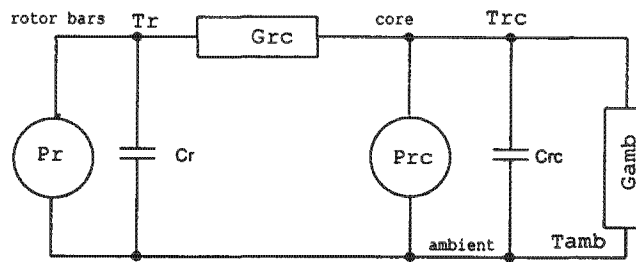


Figure 3.7: Rotor thermal model circuit

Where P_r = rotor copper loss, (W)

P_{rc} = rotor core loss

G_{rc} = thermal conductance between rotor bars and core, (W/°C)

C_r, C_{rc} = rotor thermal capacitance, (Ws/°C)

T_r, T_{rc} = rotor temperature, (°C)

3.3.2 Thermal model circuit analysis

The stator thermal model circuit in figure 3.6 can be treated like an electrical circuit. The following electrical/thermal analogies in table 3.1 are useful when analysing the thermal circuit.

Table 3.1: Electrical/Thermal analogies

Electrical circuit	Thermal circuit
Voltage (V)	Temperature (T)
Current (I)	Heat flow (power) (P)
Electrical conductance (G)	Thermal conductance (G)
Electrical capacitance (C)	Thermal capacitance (C)

The thermal circuit can be analysed by applying Kirchoff's current law (KCL) on the respective circuit nodes. Applying KCL or nodal analysis at phase A node in figure 3.6 gives:

$$-P_a + (T_a - T_b) \cdot G_{ab} + (T_a - T_c) \cdot G_{ac} + (T_a - T_h) \cdot G_{ah} + C_a \cdot \frac{dT_a}{dt} = 0 \quad (3.5)$$

Equation 3.5 can be rearranged to:

$$\frac{dT_a}{dt} = \frac{P_a - (T_a - T_b) \cdot G_{ab} - (T_a - T_c) \cdot G_{ac} - (T_a - T_h) \cdot G_{ah}}{C_a} \quad (3.6)$$

Applying nodal analysis to the remaining nodes will result to the following equations:

$$\frac{dT_b}{dt} = \frac{P_b - (T_b - T_a) \cdot G_{ab} - (T_b - T_c) \cdot G_{bc} - (T_b - T_h) \cdot G_{bh}}{C_b} \quad (3.7)$$

$$\frac{dT_c}{dt} = \frac{P_c - (T_c - T_a) \cdot G_{ac} - (T_c - T_b) \cdot G_{bc} - (T_c - T_h) \cdot G_{ch}}{C_c} \quad (3.8)$$

$$\frac{dT_h}{dt} = \frac{(T_a - T_h) \cdot G_{ah} + (T_b - T_h) \cdot G_{bh} + (T_c - T_h) \cdot G_{ch} - (T_h - T_{amb}) \cdot G_{amb}}{C_h} \quad (3.9)$$

Equations 3.6 to 3.9 contain differentials and can be solved using software packages such as Matlab or Maple. These equations can be represented by the following general equation:

$$\frac{d[T]}{dt} = [C]^{-1} \cdot ([P] - [G] [\Delta T]) \quad (3.10)$$

where [T] = temperature at each node
[C] = thermal capacitance matrix
[G] = thermal conductance matrix
[P] = heat sources at each node

In order to determine the temperature at each node using equation 3.10, the conductances, capacitances and heat source elements must be known. Stator winding loss and the core loss are heat sources and are easily calculated from the electrical model. The challenge is to determine the elements of the thermal conductance and capacitance matrices without using complex methods.

3.3.3 Thermal Model Circuit Parameter Determination

Thermal Conductance

Thermal conductance measures the ability of material to transfer heat. A low value of thermal conductance between two points will result in a high temperature differential between those two points due to high thermal resistance.

The stator thermal circuit in figure 3.6 shows seven conductance values to be calculated. Therefore seven equations are required. However, the phase-to-phase conductances are all equal and as well as the phase to core conductances. Thus, the seven unknown conductance values are reduced to three. Therefore, fewer tests are required to find the conductance values.

In order to calculate the three conductance values, three temperature values and three heat sources had to be known. The thermal conductance elements were determined under steady state conditions so that the capacitances can be assumed to be charged to their steady state values. Three stator winding temperature values T_a , T_b and T_c were obtained at the end of a test by measuring

the three winding resistances. Equation 3.11 is a formula which converts resistance to temperature and was taken from the IEEE standard 112 for motors and generators [30]. The core temperature proved hard to measure and was thus taken as the fourth unknown. The heat sources were determined during the test or eliminated depending on the type of test done.

$$T = T_o + \left(\frac{R - R_o}{R_o} \right) \cdot (T_o + k) \quad (3.11)$$

where T = temperature of the winding when R was measured, ($^{\circ}\text{C}$)

R = resistance measure during the test, (Ω)

R_o = reference resistor value measure at known temperature T_o , (Ω)

T_o = initial temperature of the winding when R_o was measured, ($^{\circ}\text{C}$)

k = 234.5 for 100% IACS conductivity copper

= 225 for aluminium, based on a volume conductivity of 62%

Tests were done on a 3 kW, 4-pole, three-phase squirrel cage induction motor. Thermocouples were inserted into the stator end-windings and slots to observe both transient and steady state temperature values and to be compared with the resistance method. The induction motor was coupled to a dc motor to provide the correct cooling.

Two simple tests were done to determine the conductance values. *Test 1*: One phase winding (phase A) of the induction motor was supplied with dc voltage at rated current. The winding was excited with the dc voltage until the temperature had stabilized. The resistance of each phase was measured and converted to temperature using equation 3.11. Phases B and C had the same temperature due to winding symmetry. Since only phase A was excited, the heat source P_a , which is the input power, was known. Heat sources P_b and P_c were zero. The core loss P_h was zero because the dc voltage was used.

From the tests performed, three heat sources were eliminated and the temperature at each phase was obtained. Figure 3.6 therefore reduces to figure 3.8 (i), which shows the conductance circuit with four unknowns. The three unknowns are: phase-to-phase conductance which is denoted by G_a , phase to core conductance G_h and core to ambient conductance G_{amb} .

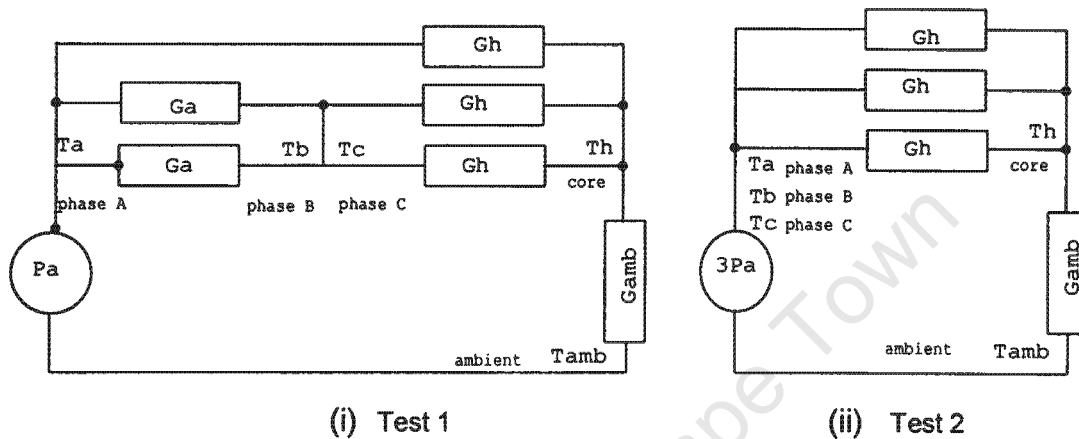


Figure 3.8: Thermal conductance circuit

Applying KCL to the three nodes in figure 3.8 (i) resulted in three equations with four unknowns, the fourth unknown being the core temperature T_h . A second test was required to get one more equation in order to calculate the conductance values.

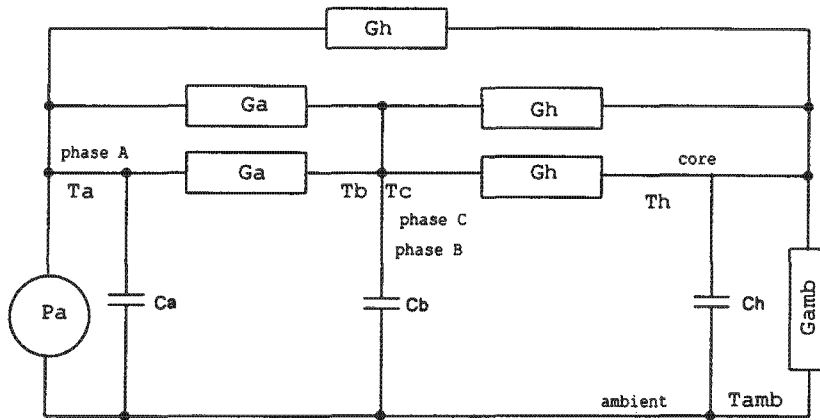
Test 2: All three phases were connected in series and then excited with dc voltage at rated motor current. The thermal circuit in figure 3.6 was reduced to figure 3.8 (ii). An additional equation was obtained, which was then used together with the other three equations from *test 1* to calculate the conductance matrix elements. Appendix C shows the calculated conductance values.

Thermal Capacitance

Thermal capacitance represents the material ability to store heat. Its value is related to the physical configuration, size and the mass of the material [21]. The transient thermal model is made possible by introducing the capacitance in the thermal circuit as shown in figure 3.6.

In order to determine the capacitance values without knowing the machine's dimensions or configuration, *test 3*, similar to *test 1* above, was performed. Stator windings were supplied with dc voltage at rated current. The temperature values in the three windings were obtained by measuring the change in the stator winding resistances as the motor heats up. Resistance values were taken until the temperature reached the final value. The heat source P_a was measured and the core loss T_h was neglected. The appropriate cooling was provided by the dc motor.

Figure 3.9 shows the circuit that was derived from figure 3.6 that led to *test 3*. In this circuit, only capacitance C_a , C_b , C_c , C_h and core temperature T_h are unknown, G_a , G_h and G_{amb} were calculated in *tests 1 and 2*. In *test 3*, only one heat source was present and the winding temperature values were obtained. The stator winding thermal capacitances were assumed to be all equal because of winding symmetry. The circuit was reduced to three equations (three nodes) with three unknowns.



Test 3

Figure 3.9: Thermal capacitance circuit

Applying KCL at phase A node gives:

$$-P_a + (T_a - T_b) \cdot 2G_a + (T_a - T_h) \cdot G_h + C_a \cdot \frac{dT_a}{dt} = 0 \quad (3.12)$$

Rearranging equation 3.12 and writing capacitance C_a as the subject of the formula resulted in:

$$C_a = [P_a - (T_a - T_b) \cdot 2G_a - (T_a - T_h) \cdot G_h] \cdot \left[\frac{\Delta t}{\Delta T_a} \right] \quad (3.13)$$

therefore, capacitance C_b and C_h is given by:

$$C_b = [(T_a - T_b) \cdot 2G_a + (T_b - T_h) \cdot 2G_h] \cdot \left[\frac{\Delta t}{\Delta T_b} \right] \quad (3.14)$$

$$C_h = [(T_a - T_h) \cdot G_h + (T_b - T_h) \cdot G_h - (T_h - T_{amb}) \cdot G_{amb}] \cdot \left[\frac{\Delta t}{\Delta T_h} \right] \quad (3.15)$$

It has been found from tests that the thermal behaviour of the motor can be modelled closely by an exponential equation with single time constant. Using the assumption that the time constant for an exponential rise curve is the time taken to reach 63% of the final value, ΔT and Δt can be obtained. These values are extracted from the temperature-time curve obtained from *test 3*. The thermal capacitance was then calculated using equations 3.13 to 3.15. Appendix C shows the calculated capacitance values.

3.3.4 Thermal Model Performance Test

The thermal model was tested by comparing the measured stator winding temperature values with the calculated values. The measured winding temperature values were taken while running a 3kW delta connected induction motor under various load conditions, unbalanced voltages, overvoltages and undervoltages.

The model inputs are the winding loss, core loss and ambient temperature. The model outputs are the winding and core temperature values. The respective motor losses were measured. These losses were fed into the thermal model and the output temperature values were compared with the measured values.

To test both the electrical and thermal models, the motor losses were calculated from the electrical model. The electrical model was given the same inputs as the actual motor. The losses from the electrical model were fed into the thermal model. The predicted temperature values were compared with the measured values, with acceptable results, to be discussed next.

Balanced Voltages

Figure 3.10 compares measured and calculated winding temperature rises under various loads. The winding temperature was measured using resistance methods and thermocouples as shown in the figure. The solid line represents the calculated values. The thermal model predicts the steady state temperature rise very closely to the measured temperature rise with a difference of less than 2°C. The transient prediction deviates slightly ($\pm 3^\circ\text{C}$) from the measured values at some loads as shown in figure 3.10.

Table 3.2 shows measured and calculated winding temperature rise during the steady state conditions.

Table 3.2: Thermal model test results under balanced voltages

Load	Winding Loss (W)	Core loss (W)	Ambient temperature °C	Measured temperature		Calculated temperature (rise) °C
				resistance (rise) °C	thermo (rise) °C	
No-load	69.6	155	21.5	19.8	19.9	19.9
Half-load	136	155	21.5	31.4	32.4	32.5
75% load	554.1	155	22.4	47.2	48.8	48.4
Full load	352.3	155	21.4	72.5	75	73

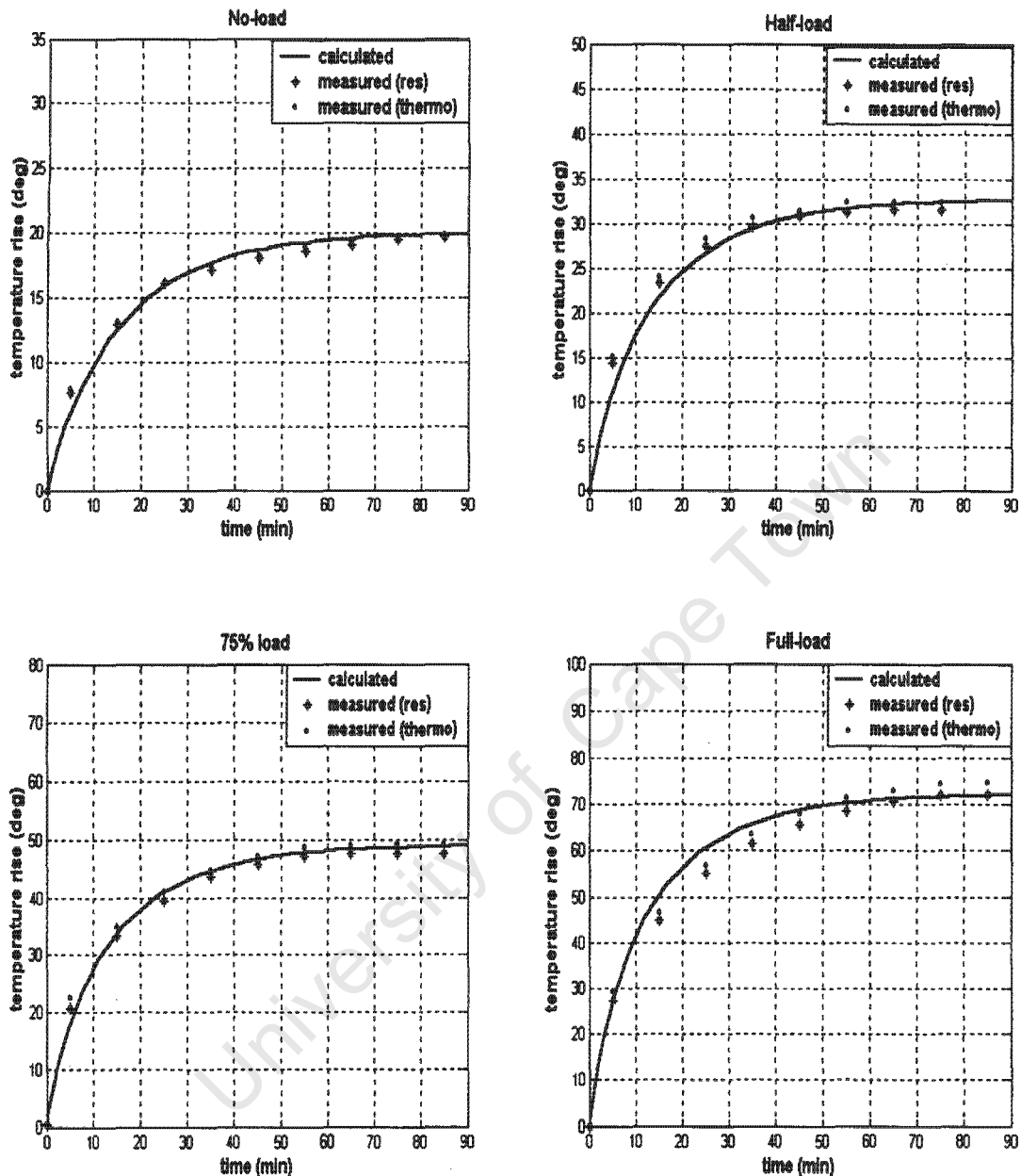


Figure 3.10: Thermal model test results under variable loads

The curves in figure 3.10 were found when the induction motor was supplied with balanced rated voltage. Thus the model works well under balanced rated voltages. The next step is to test the model under unbalanced voltages, overvoltages and undervoltages.

Unbalanced Voltages

To test the model with unbalanced voltages, the motor was supplied with rated average voltage plus 3% to 5% unbalance. At 3% unbalance, 75% load was imposed on the motor shaft. 4% and 5% unbalance tests were performed without load on the shaft. The steady state winding temperature for each phase was obtained from the measured winding resistance. The stator winding loss and core loss were calculated and fed into the model. Table 3.3 shows the comparison between the measured and the predicted temperature rise under unbalance operation. The difference is less than 2°C. Hence the thermal model works with unbalanced voltages.

Table 3.3: Thermal model test results under unbalanced voltages

Unbalance %	Load	Phase winding Loss			Core loss (W)	Measured temperature			Calculated temperature			Ambient temp °C
		A (W)	B (W)	C (W)		A °C	B °C	C °C	A °C	B °C	C °C	
3	75%	112	54.5	75.7	165	55.2	46.7	50.9	56.1	48.5	51.5	24.4
4	No-load	43.6	14.8	31.7	175	25.7	21.4	25.7	26.5	22.8	25	17.8
5	No-load	46.7	32.7	9.5	186	25.3	25.3	21.3	27.2	25.4	22.4	22.7

Overvoltages and Undervoltages

The thermal model was tested when the motor was supplied with either 10% overvoltage or 10% undervoltage, with and without unbalance at no-load and full-load respectively. Table 3.4 shows that the measured and the calculated temperature rise compare very closely. Therefore, the model works under over and undervoltage with and without unbalance voltages.

Table 3.4: Thermal model test results under over and undervoltages

Input voltage %	Unbalance %	Load	Phase winding loss			Core loss (W)	Measured temperature			Calculated temperature			Ambient temp °C
			A (W)	B (W)	C (W)		A °C	B °C	C °C	A °C	B °C	C °C	
90	0	None	13.7	13.7	13.7	114	12.8	12.8	12.8	12.8	12.8	12.8	17.8
90	0	Full	128.0	128.0	128.0	114	77.1	77.1	77.1	76.7	76.7	76.7	18.3
90	3	None	16.9	8.1	28.9	125	17.1	12.3	17.1	15.6	14.4	17.1	17.8
90	5	None	20.3	7.0	41.0	141	21.4	17.1	21.4	18.8	17.1	21.4	17.8
110	0	None	43.0	43.0	43.0	233	33.9	33.9	33.9	34.6	34.6	34.6	23.9
110	0	Full	98.2	98.2	98.2	233	63.5	63.5	63.5	65.3	65.3	65.3	23.9
110	1	None	47.0	40.5	66.4	234	36.2	36.2	36.2	38.8	37.9	41.2	17.8

Supply Voltage Magnitude Variation with Time

The thermal model was also tested under variable motor terminal voltage with time. Figure 3.11 shows the supply voltage profile that was fed into a 380V induction motor terminal. The motor was kept running at full-load for 70 minutes. The voltage was varied as follows: firstly, the motor was run at rated voltage for 10 minutes. Then, 10% overvoltage was introduced for 20 min. 10% undervoltage followed for another 20 min, the voltage was increased to rated for the next 10 min. 5% unbalance was finally introduced in the last 10 min. The winding temperature was measured at each case. The stator winding and core losses were also determined.

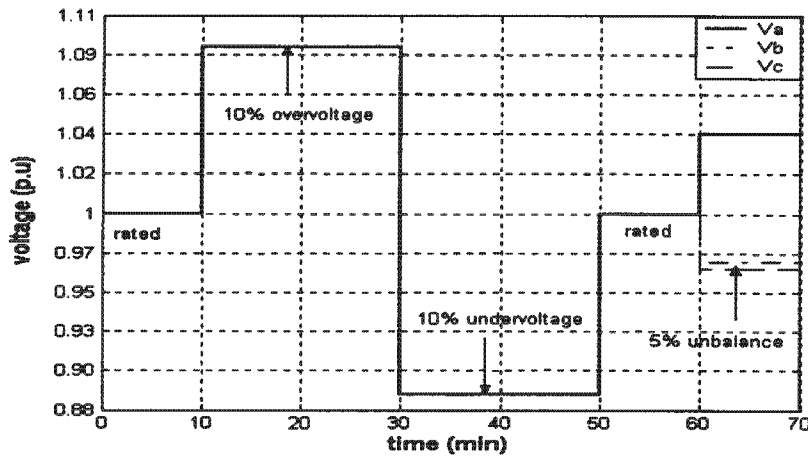


Figure 3.11: Supply voltage variation with time

Figure 3.12 compares the measured and calculated temperature values when the motor is supplied with time-varying voltage magnitudes. The winding temperature values were measured using the resistance method and thermocouples. The predicted values gave a good correlation of $\pm 3^{\circ}\text{C}$ with the measured values. The thermal model responds well to the supply voltage variation with time.

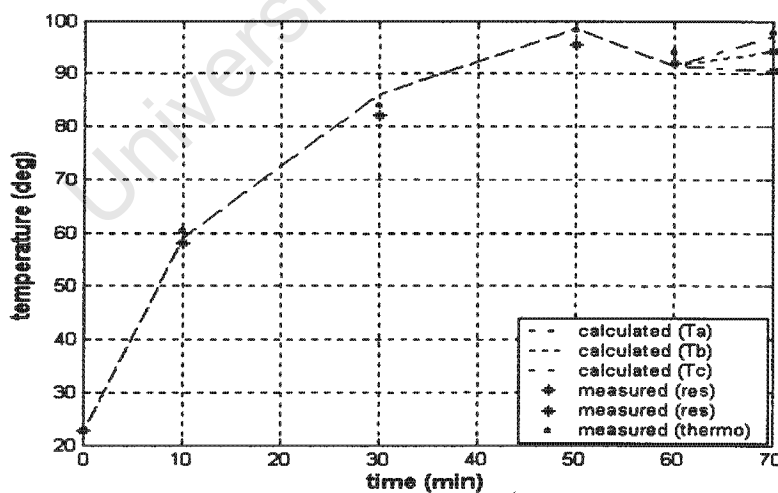


Figure 3.12: Thermal model test results under supply voltage variation

3.4 CONCLUSIONS

An induction motor electrical model was developed and tested using positive and negative sequence equivalent circuits. The stator thermal model circuit found in [21] was adopted. Simple tests were performed to determine the thermal conductance and capacitance. Both transient and steady state model performance characteristics were observed. It was concluded from the tests that the thermal model works with balanced voltages, unbalanced voltages, over and undervoltages, and also with time-varying voltage magnitudes. The assumption of separating the stator and rotor thermal circuit was justified because of the good correlation between the measured and the predicted temperature values.

4. MOTOR LIFE ESTIMATION AND DERATING

4.1 INTRODUCTION

Induction machines are designed to operate at rated conditions and have finite lifetime. Motor winding failures due to stator insulation breakdown has been found to be one of the major causes of motor failure [28]. The motor insulation life is affected by thermal, electrical and mechanical stresses, as well as environmental conditions. In this project, the thermal stress is considered to dominate other stresses. That is, the insulation ageing process will depend on the magnitude and duration of the operating temperature.

The winding insulation has a specific lifetime and it deteriorates with time due to thermal stresses. Therefore, motor life can be predicted by estimating the insulation life. The thermal ageing model that modifies the 10°C rule (insulation life is halved for every 10°C rise) to a more accurate half interval index is used to estimate motor life [18].

When a machine is supplied with balanced voltages at rated load or less, it is expected to last for its pre-defined lifetime. However, the supply voltage is not always balanced. In this chapter, motor life will be estimated when a motor is operating in the presence of over or undervoltages in combination with unbalanced voltages. In order to restore motor life under the same conditions, motor derating is also addressed.

4.2 INSULATION CLASSES

Each material has a maximum operating temperature, above which it will rapidly deteriorate. Table 4.1 shows the insulation class type, thermal limit and allowable temperature rise at an ambient temperature of 40°C.

Table 4.1: Insulation class ratings

Class	Maximum temperature °C	Temperature rise °C
A	105	65
B	130	90
F	155	115
H	180	140

4.3 THERMAL AGEING MODEL

Equation 4.1 represents the thermal ageing model. This model allows the user to estimate insulation life for all insulation classes because of its half interval index (HIC). The equation is known as the Arrhenius' equation [18]

$$L_x = L_{100} \cdot 2 \cdot e^{(T_c - T_x)/HIC} \quad \text{in (yrs, hrs, min, etc),} \quad (4.1)$$

where L_x = percent lifetime at temperature, T_x (°C)

L_{100} = percent lifetime at rated temperature, T_c (°C)

T_x = hot-spot temperature for insulation class, (°C)

T_c = total allowable temperature for insulation class, (°C)

HIC = halving interval, (°C) (14, 11, 9.3, 8 and 10 for class A, B, F, H and H' respectively)

4.4 MOTOR LIFETIME ESTIMATION

The life span of an induction motor can be estimated by using the electrical model, thermal model and Arrhenius' equation as shown by the flow-chart in figure 4.1. The supply voltage is chosen and converted to a positive sequence voltage V_p and negative sequence voltage V_n and then fed into an electrical model. The stator windings and core losses were calculated. The thermal model was supplied with these losses at a particular ambient temperature. The temperature obtained from the thermal model was used in equation 4.1 to estimate the motor life span.

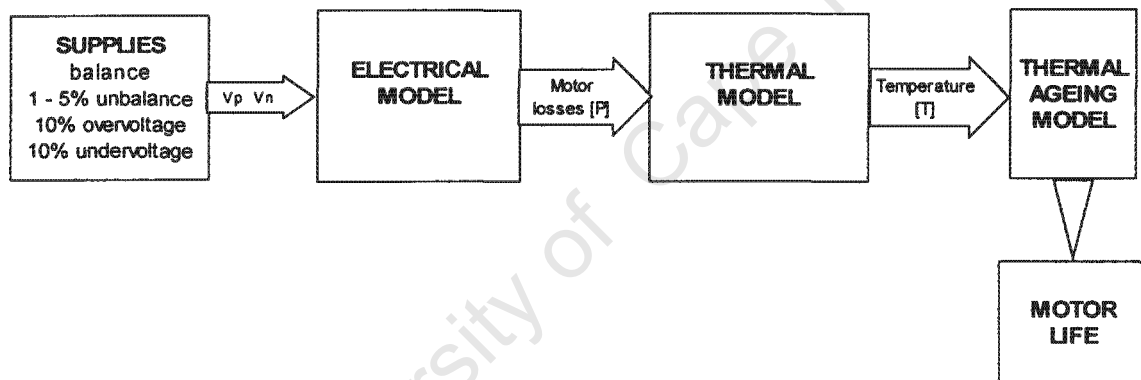


Figure 4.1: Motor life prediction flow-chart

4.4.1 Motor Life Estimation at Rated Condition

A 3kW, 50Hz, squirrel cage induction motor with class F insulation was used when performing practical tests and modelling. The motor was supplied with a 380V set of balanced voltages as shown in figure 4.2. It was run at full-load until the final temperature of 94°C at an ambient temperature of 25°C was reached.

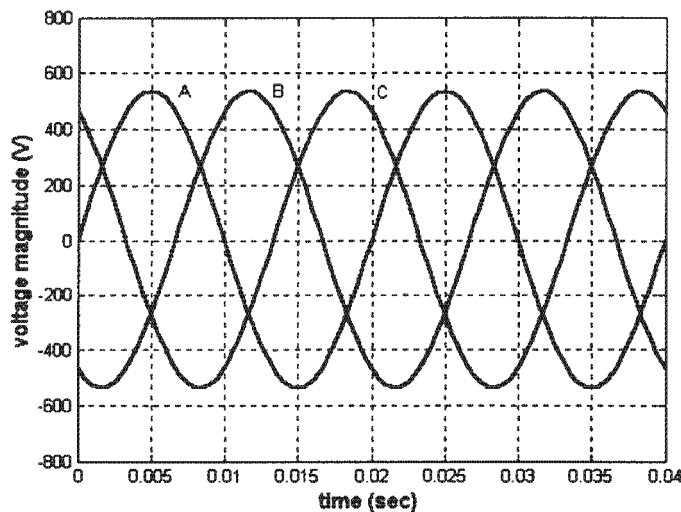


Figure 4.2: Balanced voltage waveforms

The temperature rise was found to be $(94^{\circ}\text{C} - 25^{\circ}\text{C}) = 69^{\circ}\text{C}$. This value is close to a class A temperature rise value of 65°C . This motor has a class A temperature rise with class F insulation. The use of class F insulation will prolong the motor life over a class A insulation because the class F insulation allows a temperature rise of 86°C ($155^{\circ}\text{C} - 69^{\circ}\text{C} = 86^{\circ}\text{C}$) before reaching its maximum allowable temperature limit.

The insulation class limit is normally based on 20 000 hours (2.3 years) period. That is, the insulation is expected to operate continuously at its maximum temperature for 2.3 years without failing [18, 28]. For a motor to operate for more than 2.3 yrs, the manufacturer will have to use a higher insulation class. The life will be reduced even further under unbalanced supplies.

Even if a motor has class A temperature rise with class F insulation, the insulation life will deteriorate with time. The insulation life can be estimated using class A temperature rise and then substituted to class F insulation using equation 4.2 [18].

$$\ln\left(\frac{t_r}{t_i}\right) = \frac{\varphi}{k} \cdot \left(\frac{1}{T_r} - \frac{1}{T_i}\right) \quad (4.2)$$

where t_r = time at temperature T_r

t_i = time at temperature T_i

T_r = reference temperature, (kelvin scale)

T_i = initial temperature, (kelvin scale)

$k = 0.8617 \cdot 10^{-4}$ eV/K

$\varphi = 1.05$ eV

The insulation life using class A temperature rise was found to be 43.2 times class F insulation life at an ambient temperature of 40°C. At a lower ambient temperature of 25°C, class A insulation life was 58 times that of class F. Therefore the motor will last longer at lower ambient temperatures. For example, if class F insulation life is 2.3 yrs, this motor will last for $43.2 \cdot 2.3 = 99.4$ years or $58 \cdot 2.3 = 133$ years at ambient temperature of 40°C and 25°C respectively. The motor is expected to last for these years if operated continuously at full-load at constant temperature.

4.4.2 Motor Life Estimation under Unbalanced Supplies

Figure 4.3 shows 5% voltage unbalanced waveforms. Figures 4.4 and 4.5 show 10% overvoltages and 10% undervoltages with 5% unbalanced voltages respectively. These voltage waveforms are amongst the case studies that were simulated on matlab software when estimating motor life. These waveforms show the deviation from the balanced case in figure 4.2.

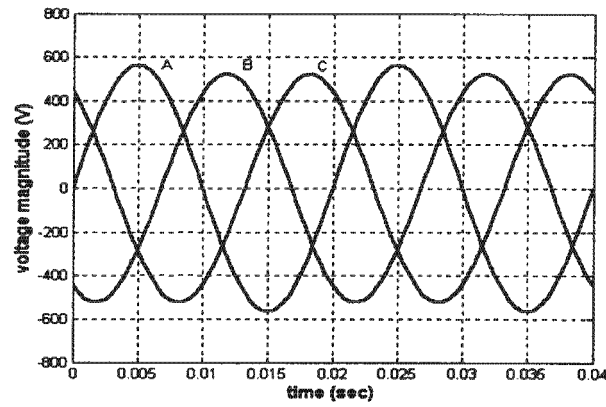


Figure 4.3: 5% unbalanced voltage waveforms

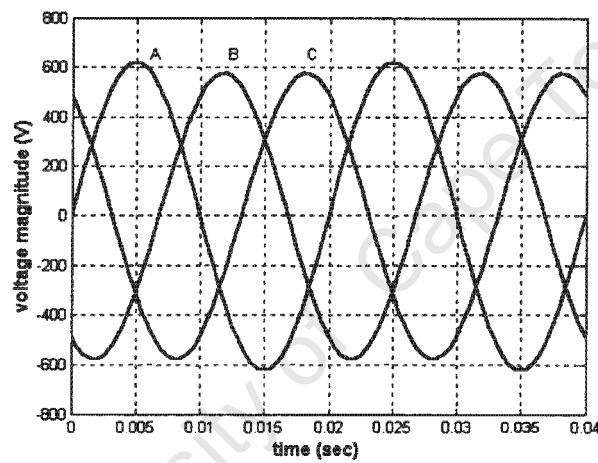


Figure 4.4: 10% overvoltage with 5% unbalanced voltage waveforms

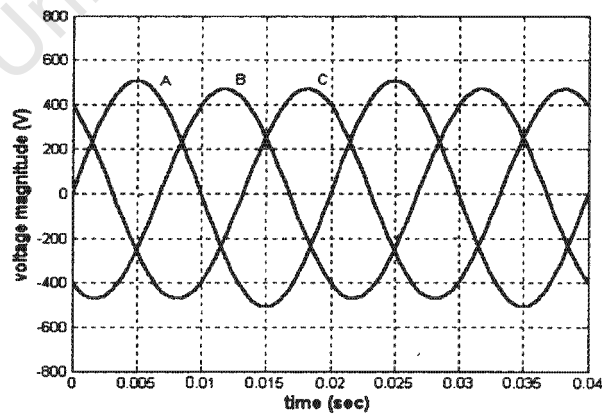


Figure 4.5: 10% undervoltage with 5% unbalanced voltage waveforms

The motor insulation life was estimated in five cases.

- **Case 1:** A motor was run at full-load with unbalanced voltages.
- **Case 2:** Its output power was derated to 95%.
- **Case 3:** The output power was derated further to 85%.
- **Case 4:** A motor was run at full-load with 10% overvoltage in combination with 0 - 5% unbalanced voltages.
- **Case 5:** A motor was run at full-load with 10% undervoltage in combination with 0 - 5% unbalanced voltages.

Figure 4.6 shows the total motor temperature curves observed from the five cases described above. The ambient temperature value was 40°C. The purpose of determining the temperature values is to use them in equation 4.1 to estimate the motor insulation life in each case.

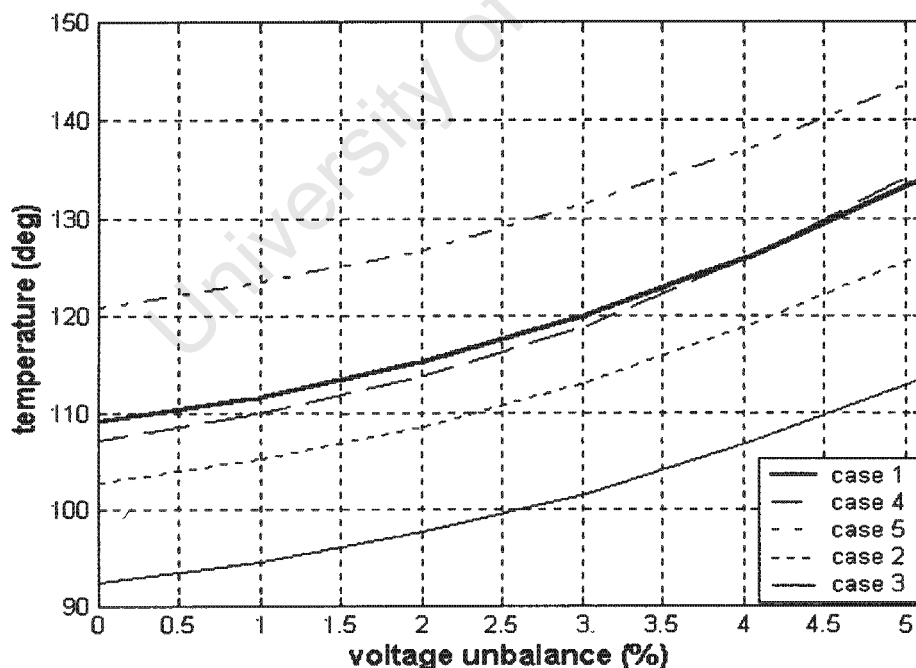


Figure 4.6: Motor winding temperature curves

Figure 4.7 (a) shows the temperature rise curves above the rated temperature of 109°C. Figure 4.7 (b) shows the respective loss of life curves. It is observed that when the motor is supplied with 10% undervoltage in the presence of unbalanced voltages at full-load, more life is lost compared to other cases. In cases 2 and 3, motor life is spared because of the derating applied. Overall, motor life is reduced as unbalanced voltage increases.

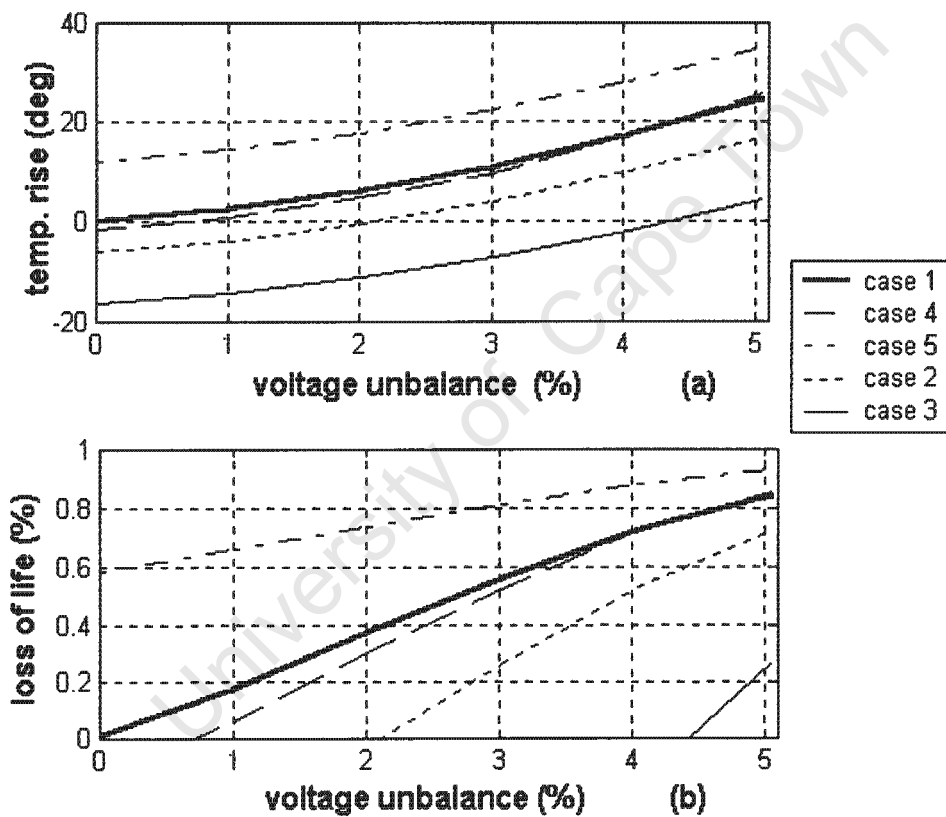


Figure 4.7: Motor winding temperature rise and loss of life curves

Table 4.2 shows the temperature rise and the respective loss of life data extracted from figure 4.7. The loss of life is in percentage of the rated life.

Table 4.2 Motor winding temperature rise and loss of life

Case	Unbalance	Temperature rise above rated °C						% Loss of life					
		0%	1%	2%	3%	4%	5%	0%	1%	2%	3%	4%	5%
1		0	3.6	8.5	14.3	21.6	30	0	16.8	36.8	55.6	72.1	83.9
2		-	-	1.6	7.0	13.8	21.8	-	-	-	26.1	52.4	71.8
3		-	-	-	-	-	7.7	-	-	-	-	-	26.8
4		-	2.0	7.1	13.1	21.5	31.1	-	6.01	30.2	51.7	72.0	85.1
5		11.8	15.8	20.5	26.5	33.3	41.4	58.5	65.8	73.5	81.3	87.6	92.6

From the example in section 4.4.1, the rated life was $43.2 \times 2.3 = 99.4$ yrs, at an ambient temperature of 40°C . If a motor is supplied continuously with case 1 voltages at 3% unbalance, a 14.3°C rise will reduce the insulation life by $0.556 \times 99.4 = 55.26$ years. Thus the motor will be expected to last for $(99.4 - 55.26) = 44.1$ years. The worst case here is when the motor is supplied with case 5 voltages plus 5% unbalance. Only 7.4 yrs [$99.4 \times (1 - 0.926)$] of life will be expected if the motor runs continuously at full-load.

Suppose a motor was operating at an ambient temperature of 25°C instead of 40°C . The rated life was estimated to be 133 years. Operating the motor with case 1 voltages plus 3% unbalance, the motor will last for $[133 \times (1 - 0.556)] = 59.1$ years, an additional of $(59.1 - 44.1) = 15$ years.

The loss of life predictions above assumes that a motor is running continuously at a constant temperature. However, motor duty cycles, supply voltages, ambient temperature, load cycles, etc, change with time. These changes will either decrease or increase motor temperature, hence the motor expected life will also change depending on the temperature magnitude. The next section presents

motor life scenarios to show how motor life is estimated when the temperature varies with time.

4.5 SCENARIOS ON MOTOR LIFE ESTIMATION

The previous section has shown that motor life can be predicted using equation 4.1 when a motor is operating at a constant temperature throughout its lifetime. In practice, motor temperature changes as the voltage or load changes, hence the motor life span. The scenarios presented here show how motor life is predicted when temperature varies with time.

Suppose a motor has a life span of 99.4 years when operated at a constant rated temperature of 109 °C (ambient of 40°C). This is the same motor used in the previous examples. Suppose this motor experiences voltage changes shown in table 4.3 during the course of its life:

Table 4.3: Motor voltage and temperature variation with time

Case	Unbalance %	Undervoltage %	Rated %	Overvoltage %	Load %	Time years	Temperature °C
1	0	0	100	0	100	5	109.01
2	2	10	0	0	100	2	129.58
3	5	0	0	10	100	1	140.11
4	5	0	100	0	100	2	139.09
5	3	0	100	0	100	5	123.34
6	2	0	0	10	100	5	116.16
7	4	10	0	0	90	2	122.05

By looking into the temperature column, one can see that the motor life will be reduced below the rated life of 99.4 yrs because the temperature values from case 2 to case 7 exceed the rated value of 109 °C. The challenge is to estimate the life lost in each case.

Figure 4.8 shows how the winding temperature changes with time. This graph was plotted using the data obtained in table 4.3. The purpose here is to estimate how much life is lost in the each case and then find the overall life reduction.

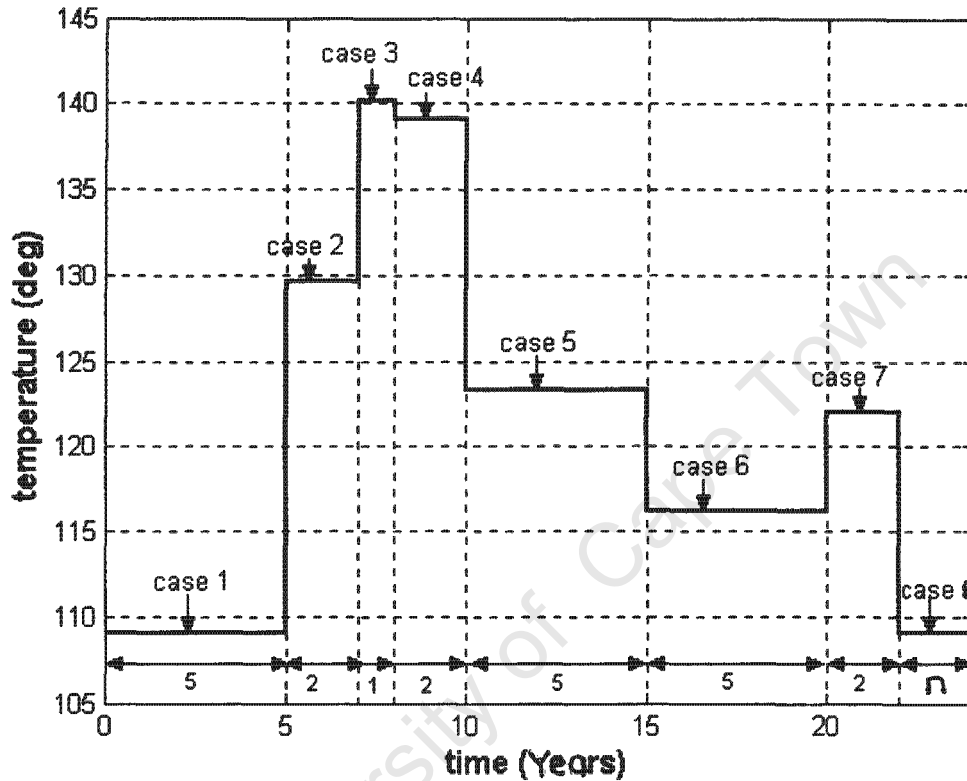


Figure 4.8: Motor winding temperature change with time

Applying equation 4.1 in each case gives the expected insulation life for that case but assumes that the motor is operating continuously at that temperature throughout its life span. For example, the expected life in case 5 using this equation is 34.2 years and $(99.4 - 34.2) = 64.9$ years is lost. This equation does not give the life lost for those five years of operation in relation to the rated life. The solution to this problem is to find the deterioration rate at that period and then calculate the life lost as a function of operation time.

If a motor is operating at constant temperature throughout, the insulation life will deteriorate at a particular rate. As the temperature changes with time, the deterioration rate will also change. Dakin found that the rate of deterioration is inversely proportional to time to reach a particular deterioration condition [34]. That is, the deterioration rate can be found by taking the reciprocal of the time taken to reach the end of life.

Insulation life is predicted in each case by finding the respective deterioration rate as follows. In case 1, the motor is operated at rated temperature for 5 years. The deterioration rate is given by $\frac{1}{L_x}$, where L_x is the expected life found using equation 4.1. Since the motor life span of 99.4 years at rated temperature has been determined, operating for 5 years at rated temperature will lead to a loss of 5 years. This is confirmed by finding the rate of deterioration $1/L_x = 1/99.4 = 0.01$ (1/years). The product of the deterioration rate, rated life and the number of operating years gives the life lost, which in this case is $(0.01*99.4)*5 = 5$ years. The rated life will be used as reference.

In case 2, the temperature rises to 129.58 °C. The deterioration rate increased to 0.0466. Operating for 2 years at this temperature reduced the life further by $(0.0466*99.4)*2 = 9.27$ years. Table 4.4 shows the insulation life lost in all cases. In cases 2 to 7, the rate of deterioration increased due to the increase in temperature above rated.

Table 4.4: Deterioration rate and Loss of life

Case	Operation time years	Temperature °C	Rate 1/years	Loss of life years
1	5	109.0	0.0101	5.0
2	2	129.6	0.0466	9.3
3	1	140.1	0.1022	10.2
4	2	139.1	0.0948	18.8
5	5	123.3	0.0293	14.6
6	5	116.2	0.0172	8.5
7	2	122.1	0.0266	5.3

The total life lost in 22 years of operation is equal to the sum of the life lost in each case. That is, 71.6 years of life is lost after 22 years of operation and $n = (99.4 - 71.6) = 27.8$ years is left. Alternatively, the total life lost can be found by calculating the average deterioration rate over the period of 22 years.

Suppose a motor is subjected to the temperature changes as shown in figure 4.9 for 24 hours. These temperature changes could have been caused by overloading the motor or by voltages change mentioned in table 4.3. The life reduced in a day is estimated by calculating the average rate of deterioration. The average deterioration rate calculated from figure 4.9 is 0.031. Therefore the life lost in a day will be $(0.031 \times 99.4) \times 24 = 73.6$ hours, which is equivalent to 3 days. If the motor continues to operate with this temperature profile, it will be expected to operate for $L_x = 1/0.031 = 32.3$ years.

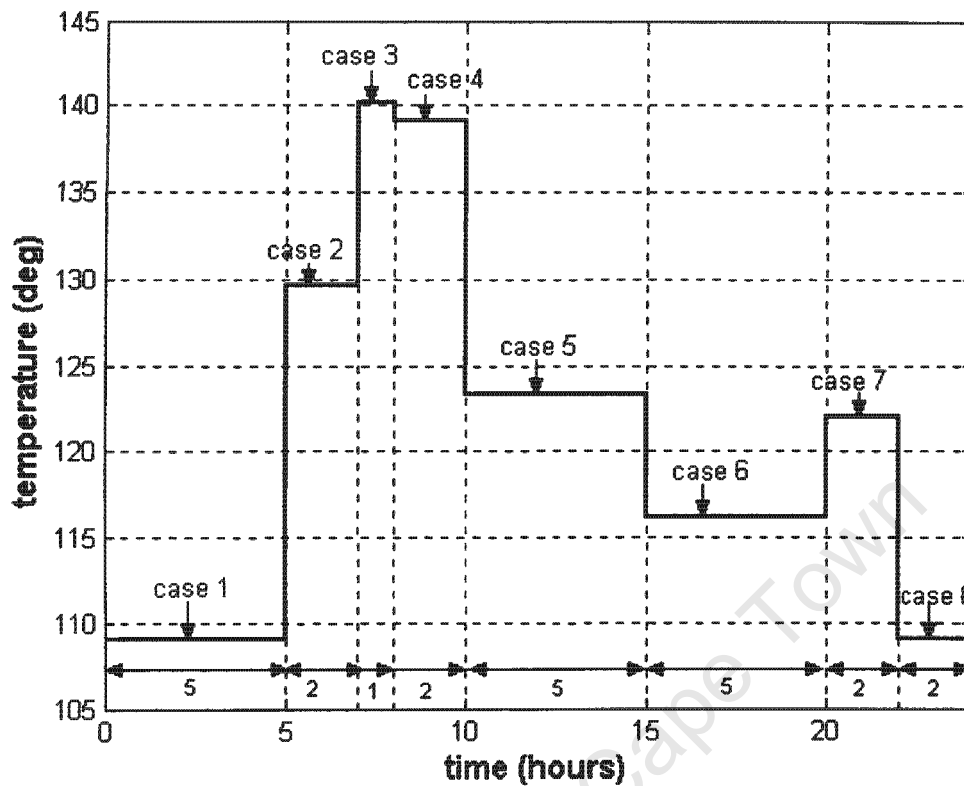


Figure 4.9: Motor winding temperature change within 24 hours

Motor life was estimated for continuous motor operation at constant temperature and also when the temperature changes with time. It has been shown that motor life is reduced as the temperature increases above rated. The solution to avoid the loss of useful motor life is to keep the temperature at rated or below. The simplest protection is to reduce the motor output power to keep the temperature rated. This is called motor derating.

The existing NEMA derating curve works for unbalanced voltages assuming rated average voltage. Since overvoltages and undervoltages occur in the power system and reduce motor life, it makes sense to include them in the derating curve to restore life. The development of new derating curves that includes a combination of over or undervoltage with unbalance is explained next.

4.6 DEVELOPMENT OF NEW DERATING CURVES

The flow chart in figure 4.10 shows the steps that were followed to develop the derating of the motor. An electrical model was used to calculate motor losses due to unbalance voltages in combination with over or undervoltages. The thermal model predicted the corresponding temperature and the derating factor was obtained.

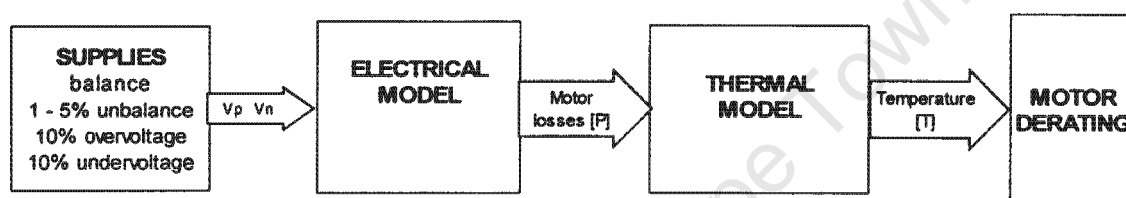


Figure 4.10: Motor derating flow-chart

The derating curves in figure 4.11 were developed by running the following three cases:

- **Case 1:** A motor was supplied with unbalanced voltages at rated average voltage.
- **Case 2:** A motor was supplied with 10% overvoltage in combination with voltage unbalance up to 5%.
- **Case 3:** A motor was supplied with 10% undervoltage in combination with voltage unbalance up to 5%.

The first procedure when determining derating curves was to calculate the motor rated temperature at full-load when supplied with balanced rated voltages. The chosen voltages were applied at the motor terminals. The highest stator winding temperature was calculated assuming that the motor was operating at full-load. The temperature was found to be more than the rated. The motor output power was reduced so as to keep the temperature at rated. The derating factor was determined as the ratio of the calculated output power to the rated power.

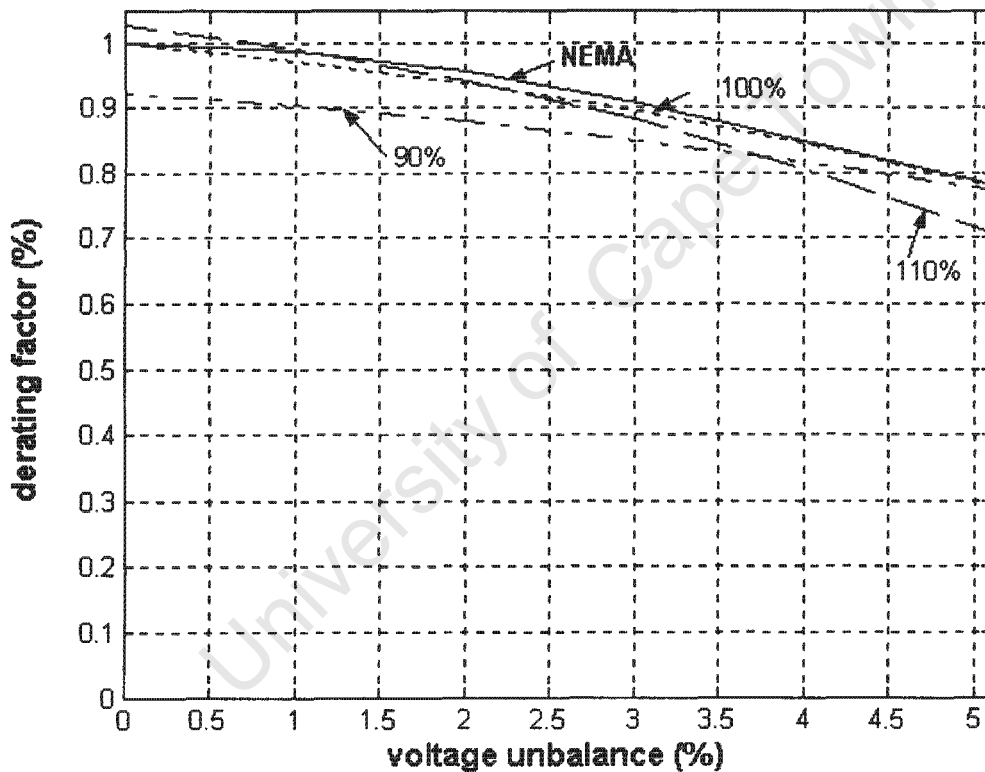


Figure 4.11: New derating curves

The 100% curve in figure 4.11 shows the derating curve required to protect the motor when supplied with case 1 voltages. This curve is very close to the NEMA curve as expected. The 110% curve is the derating curve that can be used to protect the motor when supplied with 10% overvoltages in combination with unbalance voltages. The beginning of the 110% curve suggests that the motor can take a little bit of overload before going above the rated temperature. Thus below 1% unbalance, the motor can be operated at full-load without being derated. This is the same as for the NEMA derating curve. At 5% unbalance, the motor cannot be operated above 71% of the rated power.

The 90% curve in figure 4.11 shows the derating curve that will protect the motor winding from overheating when a motor is operated with a combination of unbalanced voltages with 10% undervoltage. If a motor is expected to run at full-load in the presence of undervoltage, with or without voltage unbalance, motor derating is necessary as shown by the curve.

The undervoltage and the rated voltage curves have almost the same derating at 5% unbalance. This is believed to be due to the higher I^2R and lower core losses in the undervoltage case cancelling out with the lower I^2R and higher core losses for the rated case, hence giving the same derating at that point. The core loss for the 110% curve is the highest.

4.7 CONCLUSIONS

Motor life was estimated for continuous operation at constant temperature throughout its life span and for time-varying temperature. The use of class F insulation with class A temperature rise allows longer insulation life, as long as the motor winding temperature is kept at class A rise. Motor life is reduced below rated when the rated temperature is exceeded. This is the case as motors are sometimes overloaded to produce more output, or supplied with a combination of

over or undervoltages with unbalanced voltages while loaded. The ambient temperature has an important effect on motor life. That is, operating a motor at an ambient temperature of 25°C will result in longer life when compared to one operating at 40°C.

New derating curves, which include a combination of over or undervoltages with unbalanced voltages, were developed. New derating curves provide guidelines on how to derate a motor to avoid overheating and loss of life when the motor is operating in the presence of voltage unbalance with a combination of overvoltage or undervoltage.

University of Cape Town

Chapter 5

5. CONCLUSIONS AND RECOMMENDATIONS

5.1 CONCLUSIONS

Based on the findings presented in this report, the following conclusions are drawn:

5.1.1 Definitions of Voltage Unbalance

The definitions of voltage unbalance developed by NEMA, IEEE and IEC have been examined. The IEEE uses a similar definition of voltage unbalance as NEMA, the only difference being that the IEEE uses phase voltages rather than line-to-line voltages. The phase angle information for these two definitions is lost since only magnitudes are considered. The IEC definition, referred to as the 'true' definition, involves both magnitude and angles when calculating the positive and negative sequence voltage components. Two formulas that avoid the use of complex algebra were also presented.

An analysis was done to show the relationship between the definitions of voltage unbalance. It was found that for a given NEMA unbalance, there is a range of unbalance based on the true definition. The true definition and one of the approximation formulas have the same % unbalance for the same set of unbalanced voltages. Below 5% unbalance, the true definition and the approximation formula agree very closely. However, as the voltage unbalance increases above 5%, based on NEMA, the approximation formula starts to deviate slightly from the true definition. The true definition and the approximate formula have almost the same deviation range from the NEMA definition. At 5% unbalance, based on NEMA unbalance, the maximum deviation between the NEMA definition and the true definition is 0.8%. The difference is higher for more

extreme values of % unbalance based on the NEMA definition. It was found through motor testing that the true definition of voltage unbalance can be used on the NEMA derating curve. This allows for the use of positive and negative sequence equivalent circuits when derating the motor based on the NEMA curve. The analysis performed on the definitions of voltage unbalance helps the reader understand the differences in the definitions.

5.1.2 Electrical and Thermal Models

An electrical model of an induction motor was developed and tested using positive and negative sequence equivalent circuits. The core losses when a motor is supplied with unbalanced voltages, in combination with over or undervoltages were obtained experimentally. The core losses increase with unbalanced voltages and overvoltages.

Separate stator and rotor thermal model circuits were adopted. Simple tests were performed to determine thermal parameters from tests rather than from motor design data. The developed thermal model was able to predict both transient and steady state temperatures to a reasonable accuracy, the maximum deviation from the measured values being $\pm 3^{\circ}\text{C}$ during transients and less than 2°C in the steady state. From the model performance test, it was concluded that the thermal model works with balanced voltages, unbalanced voltages, over and undervoltages, and also with time-varying voltage magnitudes. The separation of the stator and rotor thermal circuits was justified because of the good correlation between the measured and the predicted temperature values.

5.1.3 Motor Life Estimation and Derating

The definitions of voltage unbalance, electrical and thermal models, and the thermal ageing equation were used to estimate the motor insulation life and

appropriate derating. The motor was supplied with a combination of over or undervoltages with unbalanced voltages. Motor life was estimated for continuous operation at constant temperature throughout its life span and for time-varying temperatures. Motor life is reduced when the rated temperature is exceeded.

The use of class F insulation with class A temperature rise, allows longer insulation life. The ambient temperature has an important effect on motor life. That is, operating a motor at an ambient temperature of 25°C will result in longer life when compared to one operating at 40°C.

New derating curves, which include a combination of over or undervoltages with unbalanced voltages, were developed. The NEMA derating curve was extended to include new curves as shown in figure 4.11. New derating curves provide guidelines on how to derate a motor to avoid overheating and loss of life when the motor is operating in the presence of voltage unbalance with a combination of over or undervoltages.

5.2 RECOMMENDATIONS

Based on the findings and conclusions presented in this report, the following recommendations are made:

5.2.1 Definitions of Voltage Unbalance

For voltage unbalance below 5%, the IEC or the true definition of voltage unbalance can be used on the NEMA derating curve.

5.2.2 Electrical and Thermal Models

The positive and the negative sequence equivalent circuits should be extended to include harmonics. The rotor thermal model should also be developed from simple tests.

5.2.3 Motor Life Estimation and Derating

The effects of motor startups, motor sizes and harmonics on motor life and derating should be investigated.

University of Cape Town

REFERENCES

- [1] J.E Williams," Operation of 3-Phase Induction Motors on Unbalanced Voltages", *AIEE Trans. Power Apparatus and Systems*, Vol. 73, pt III, pp. 125-133, Apr. 1954
- [2] B.N Gafford, W.C Duesterhoeft, JR and C.C Mosher III," Heating of Induction Motors on Unbalanced Voltages", *AIEE Trans. Power Apparatus and Systems*, Vol. 78, pt III-A, pp. 282-297, June 1959
- [3] M.M Berndt and N.L Schmitz," Derating of Polyphase Induction Motors Operated with Unbalanced Line Voltages", *AIEE Trans. Power Apparatus and Systems*, Vol. 81, pp. 680-686, Feb. 1963
- [4] L.L Gleason and W.A Elmore," Protection of 3-Phase Motors Against Single-Phase Operation", *AIEE Trans. Power Apparatus and Systems*, Vol. 77, pp. 1112-1120, Dec. 1958
- [5] E. Muljadi, R. Schiferl and T.A Lipo," Heating of Induction Motors on Unbalanced Voltages", *AIEE Trans. Power Apparatus and Systems*, Vol. 78, pt III-A, pp. 282-297, June 1959
- [6] W.T Martiny, R.M McCoy and H.B Margolis," Thermal relationships in an Induction Motor under normal and abnormal operation", *AIEE Trans. Power Apparatus and Systems*, Vol. 80, pt III, pp. 66-76, Apr.1961
- [7] N. Rama Rao and P.A.D Jyothi Rao," Rerating Factors of Polyphase Induction Motors Under Unbalanced line Voltage Conditions", *IEEE Trans. Power Apparatus and Systems*, Vol. 87, No. 1, pp. 240-249, Jan. 1968

-
- [8] J.R Linders," Effects of Power supply Variations on AC Motor Characteristics", *IEEE Trans. on Industry Applications*, Vol. 1A-8, No. 4, pp 383-400, July/August 1972.
- [9] R.F Woll," Effect of Unbalanced Voltage on the Operation of Polyphase Induction Motors", *IEEE Trans. on Industry Applications*, Vol. 1A-11, pp. 38-42, Jan/Feb 1977
- [10] R.G Harley and M.A Tshabalala, " Induction motor behaviour in the presence of unbalanced supply voltages", *SAIEE Trans*, June 1985.
- [11] Ching-Yin Lee," Effects of Unbalanced Voltage on the Operation Performance of a Three-phase Induction Motor", *IEEE Trans. on Energy Conversion*, Vol. 14, No. 2, June 1999.
- [12] W.H Kersting and H. Phillips," Phase Frame analysis of the Effects of Voltage unbalance on Induction Machines", *IEEE Trans. on Industry Applications*, Vol. 33, No. 2, March/April 1997.
- [13] P.B Cummings, J.R Dunki-Jacobs and R.H Kerr," Protection of Induction Motors Against Unbalanced Voltage Operation", *IEEE Trans. on Industry Applications*, Vol. IA-21, No. 4, May/June 1985.
- [14] E Muljadi, R Schiferl and T.A Lipo," Induction Machine Phase Balancing by Unsymmetrical Thyristor Voltage Control", *IEEE Trans. on Industry Applications*, Vol. IA-21, No. 4, May/June 1985.
- [15] W.H Kersting," Causes and Effects of Unbalance Voltages Serving an Induction Motor", *IEEE Trans. on Industry Applications*, Vol. 37, No. 1, March/April 2001.

- [16] M.G Say, "Alternating Current Machines", Fourth Edition, 1976.
- [17] H Oraee and A.E Emanuel, "Induction Motor Useful and Power Quality", *IEEE Power Engineering Review*, pp 47 - 48, January 2000.
- [18] E. L Brancato, "Estimation of Lifetime Expectancies of Motors", *IEEE Electrical Insulation Magazines*, Vol.8, No. 3, May/June 1992.
- [19] J. Oyama, F. Porfumo, E. Muljadi and T.A Lipo, "Design and Performance of a Digitally Based Voltage Controller for Correcting Phase Unbalance in Induction Machines", *IEEE Trans. on Industry Applications*, Vol. 26, No. 3, pp. 425-433, May/June 1990
- [20] J.F Heidbreder, "Induction Motor Temperature Characteristics", *AIEE Trans. Power Apparatus and Systems*, Vol. 77, pt III, pp. 800-804, Oct. 1958
- [21] O.C.N Souto, J.C de Oliveira, L.M Neto, "O Impacto da Qualidade da Energia no Comportamento Termico e na Vida Util de Motors de Inductao Trifasicos", *Seminario Brasileiro sobre Qualidade da Energia Eletrica*, 08 a 12 de agosto de 1999.
- [22] J. Xypteras and V. Hatzathanassiou, "Thermal Analysis of an Electrical Machine Taking into Account the Iron Losses and the Deep-Mar Effect", *IEEE Trans. on Energy Conversion*, Vol. 14, No. 4, December 1988
- [23] S.T. Zocholl, E.O Schweitzer and A.A. Zegarra, "Thermal protection of induction motor enhanced by interactive and thermal models", *IEEE trans. on Power Apparatus and Systems*, Vol. PAS-103, N0. 7, July 1984.

-
- [24] A.H. Eltom and N.S. Moharari, " Motor Temperature Estimation Incorporating Dynamic Rotor Impedance", *IEEE trans. on Energy Conversion*, Vol. 6, NO. 1, March 1991.
- [25] P.H. Mellor, D. Roberts and D.R Turner, " Lumped Parameter Thermal Model for Electrical Machines of TEFC design", *IEE Proceedings-B*, Vol. 138, No. 5, September 1991.
- [26] A.H Bonnett and G.C Soukup, " NEMA Motor-Generator Standards for Three-Phase Induction Motors", *IEEE Industry Application Magazine*, May/June 1999.
- [27] J.D. Glover and M. Sarma, "Power System Analysis and Design ", Second edition.
- [28] Engelmann R.H. and Middendorf W.H., "Handbook of Electric Motors", 1995.
- [29] ANSI/NEMA Standard MG1 -1993, "Motors and Generators".
- [30] IEEE Standard 112, 1991, "IEEE standard Test Procedure for Polyphase Induction Motors and Generators",
- [31] NRS 048-1: 1996
- [32] P.C. Sen, "Principles of Electric Machines and Power Electronics", Second Edition,
- [33] McPherson, "Introduction to Electrical machine and Transformers"

- [34] T.W. Dakin," Electrical Insulation Deterioration Treated as a Chemical Rate Phenomenon", *AIEE Trans. Power Apparatus and Systems*, Vol. 67, pp. 113 - 122, 1948
- [35] E.L. Brancato," A Pathway to Multifactor Aging", *IEEE Trans. on Electrical Insulation*, Vol. 28, No. 5, October 1993.

University of Cape Town

APPENDIX A

EXPERIMENTAL SETUP

Three-phase Induction motor nameplate ratings

Power = 3 kW
Voltage = 380 V
Current = 6.9 A
Poles = 4
Frequency = 50 Hz
Connection = Δ
Insulation class = F

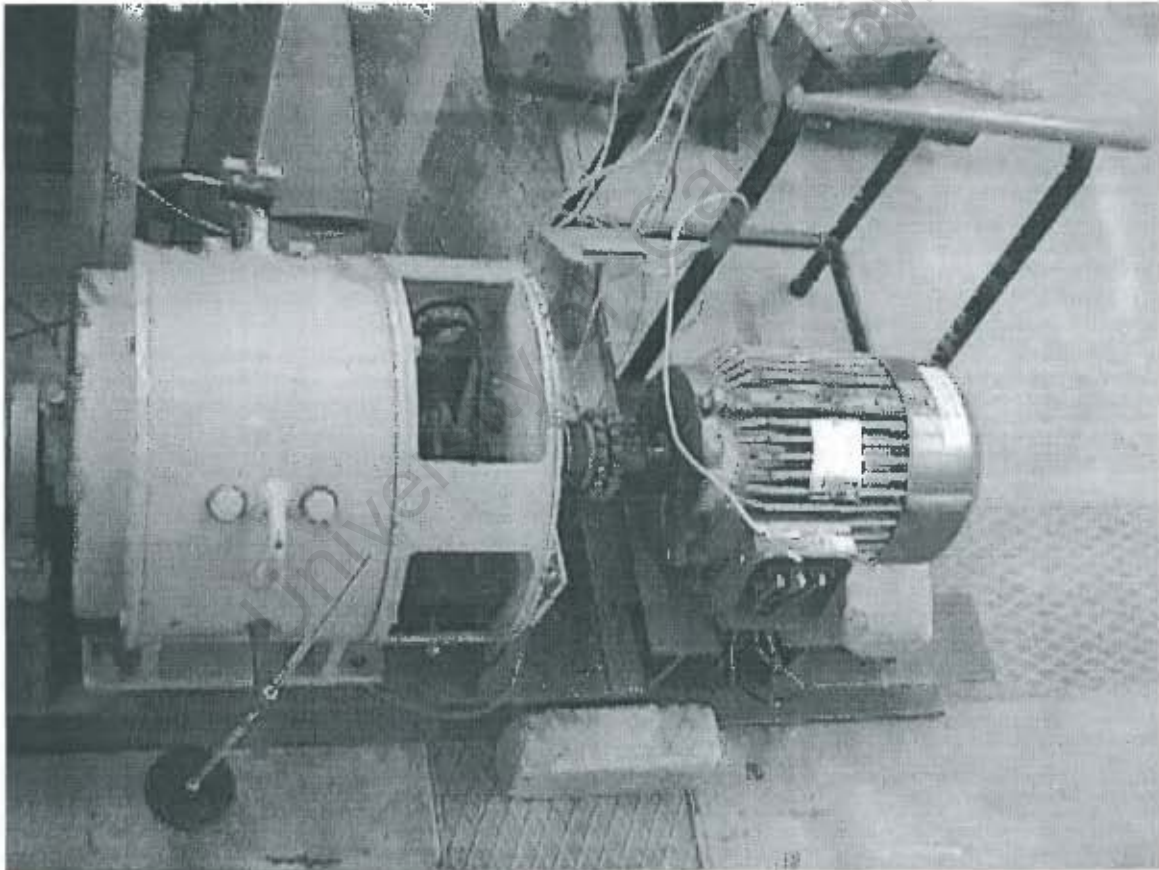


Figure A: Induction motor coupled to a dc generator.

APPENDIX B

ELECTRICAL MODEL CIRCUIT PARAMETERS

Table B-1: No-load and locked rotor tests

No-load test	Locked rotor test
Line voltage = 380.4 V	Line voltage = 52 V
Line current = 3.35 A	Line current = 6.84 A
3 phase power = 256 W	3 phase power = 530 W

Table B-2: Positive and negative sequence equivalent circuit parameters

Positive sequence circuit (Ω)	Negative sequence circuit (Ω)
$R_1 = 6.4$	$R_1 = 6.4$
$X_1 = 5.59$	$X_1 = 5.59$
$X_m = 189.8$	$X_m = 189.8$
$R'_2 = 5.14$	$R'_2 = 6.5$
$X'_2 = 8.34$	$X'_2 = 7.88$

APPENDIX C

THERMAL MODEL CIRCUIT PARAMETERS

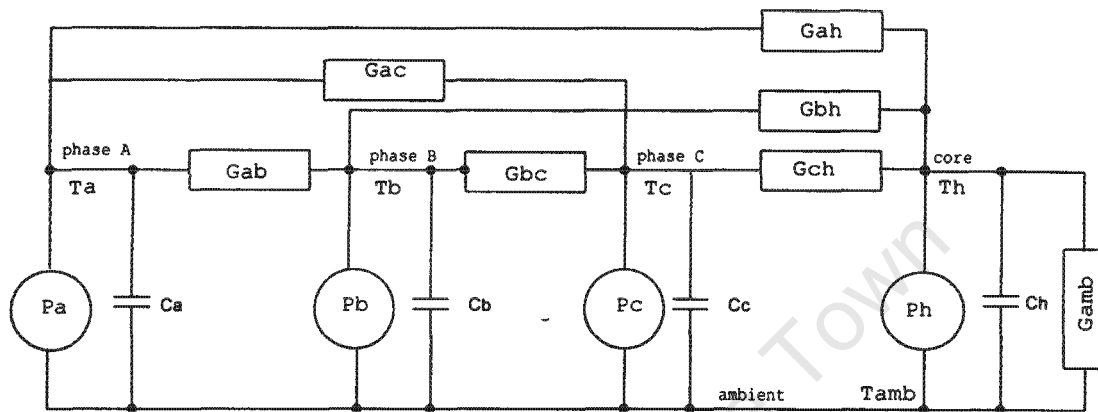


Figure C: Stator thermal model circuit

Thermal Parameters

Phase-to phase conductances, G_{ab} , G_{bc} and $G_{ac} = 2.01 \text{ W/}^\circ\text{C}$

Phase to core conductances, G_{ah} , G_{bh} and $G_{ch} = 2.38 \text{ W/}^\circ\text{C}$

Winding capacitances, C_a , C_b and $C_c = 16.2 \text{ W.min/}^\circ\text{C}$

Core capacitance, $C_h = 99.4 \text{ W.min/}^\circ\text{C}$

Core to ambient conductance, $G_{amb} = 7.275 \text{ W/}^\circ\text{C}$

BIOGRAPHY

Marubini Manyage was born in Venda, South Africa in 1978. He received the B.S. degree in electrical engineering from the University of Cape Town, South Africa in 1999. He visited Clarkson University in Potsdam, New York as a research assistant from August to December 2000. He is a member of the South African Engineering Council. He is currently working for Koeberg Nuclear Power station in Cape Town, South Africa. His field of interest is Electric Machines and Drives.